NASA CONTRACTOR REPORT

NASA CR-320

STABILITY ANALYSIS OF RELAY-CONTROL SYSTEMS VIA THE DIRECT METHOD OF LYAPUNOV

by Stein Weissenberger

Prepared under Grant No. NsG-133-61 *by*
STANFORD UNIVERSITY
Stanford, Calif.
for

NATIONAL AERONAUTICS AND SPACE ADMINISTRATION • WASHINGTON, D. C. • OCTOBER 1965

NASA CR-320

STABILITY ANALYSIS OF RELAY-CONTROL SYSTEMS VIA THE DIRECT METHOD OF LYAPUNOV

By Stein Weissenberger

Prepared under Grant No. NsG-133-61 by
STANFORD UNIVERSITY
Stanford, Calif.

for

NATIONAL AERONAUTICS AND SPACE ADMINISTRATION

For sale by the Clearinghouse for Federal Scientific and Technical Information
Springfield, Virginia 22151 – Price $3.00

ABSTRACT

This thesis presents a new computational technique for constructing Lyapunov functions for estimating the domain of asymptotic stability of non-linear control systems. A machine program assigns figures of merit (based on the size of the stability-boundary estimates) to the members of a set of Lyapunov functions and then searches for the one which maximizes this measure. The method is applicable to a wide variety of non-linearities but it is principally applied in this thesis to relay-control systems, which are not tractable by other systematic techniques such as the method of Zubov. The numerical results of a number of second- and third-order examples are presented, including one example with non-linear plant dynamics and one example with a saturation characteristic in place of the relay.

The thesis is broadly divided into two parts. The first part contains a discussion of the motions of relay-control systems and the technique of investigating their stability domains with Lyapunov functions. The second part contains a discussion of existing methods of generating Lyapunov functions and a description of the new method, along with the examples.

The method of constructing Lyapunov functions demonstrates marked advantages in that it is not limited to second-order systems, it is not restricted to smooth or even continuous non-linearities, and it effectively utilizes the resources of high-speed machine computation.

ACKNOWLEDGMENTS

The author expresses his thanks to Dr. I. Flügge-Lotz for her guidance and encouragement during the course of this research and to Dr. J. V. Breakwell and Dr. R. E. Kalman for their helpful criticism of the manuscript. He also wishes to thank Dr. J. J. Rodden for his advice and assistance, particularly with problems of numerical computation. This work was performed in association with research sponsored by the National Aeronautics and Space Administration under Research Grant NsG-133-61 and was partially supported by the General Research Program of Lockheed Missiles and Space Company. Computer time was made available at the Stanford Computation Center by research grant No. NSF-GP948 of the National Science Foundation.

TABLE OF CONTENTS

LIST OF FIGURES

LIST OF FIGURES (Continued)

I. INTRODUCTION

The direct method of Lyapunov is a technique for investigating the stability of a system of non-linear, ordinary differential equations. [1], [2],[3]* In theory the method is quite simple and general; it consists essentially of forming a sign – definite scalar function of the system's state and examining for definiteness the sign of the time rate of change of this function along the system's trajectories. Because of its elegance, the direct method has been the subject of much research in recent years. It was originally hoped that it would provide a powerful means of studying the stability properties of non-linear control systems. Considerable experience, however, has shown that the application of the method is far from simple and that success frequently depends on the skill and persistence of the user.

An important practical application of the direct method which currently suffers notably from these defects is the estimation of the domain of asymptotic stability, the set of initial system states which with increasing time return to a desired equilibrium state in a certain well-behaved fashion. The particular problems that arise are twofold: First, the numerical testing of a Lyapunov function to determine the boundary of the estimate is involved and in general not feasible to perform by hand in realistic examples. Second, there is no general method for systematically constructing Lyapunov functions to improve stability domain estimates. A solution to the first problem was recently found by Rodden [4] when he developed and used numerical techniques to determine stability boundaries for a wide variety of non-linear control systems. Although much effort has been expended on the second problem, no entirely satisfactory solution has been found.

Of the techniques which have been developed for generating Lyapunov functions, the only direct and truly systematic one is the method of Zubov. [5] However, one of its chief defects is that it is not applicable to discontinuous systems. The subject of this thesis is a new, systematic technique for obtaining useful estimates of the domain of asymptotic

*Numbers in brackets refer to the bibliography at the end of the report.

stability for relay-control systems, an important class of systems whose discontinuous nature excludes them from the treatment by Zubov's method. This new technique utilizes as a basis the numerical procedure employed in Reference [4] for determining the boundary of the estimate; an "optimum" estimate of the stability boundary is computed numerically by systematically searching for the best Lyapunov function within a specified class, the functions being ranked according to the size of their stability-boundary estimates.

Although this technique was developed to overcome special problems connected with discontinuous systems, it is applicable to systems with continuous non-linearities as well. It is hoped that though this thesis will be principally devoted to the study of relay-control systems, the examples will also serve as a kind of case-study for the application of the technique to other classes of non-linear control systems. Some possible extensions of the method will be outlined and, in addition, the extension of the method to systems with a saturation type non-linearity will be discussed in detail.

This problem divides itself naturally into two basic parts. The first part consists of the development of the technique of analyzing Lyapunov functions for relay-control systems. In Chapter II the relay-control system is defined and its special motions are qualitatively described and classified. It is then shown in Chapter III how to apply a special class of Lyapunov functions to these systems; the conditions for the existence of these Lyapunov functions are also discussed. The second and major part of the thesis concerns the construction of Lyapunov functions for producing useful stability boundary estimates. In Chapter IV existing methods are discussed and the new technique for improving the estimate employing the class of functions introduced in Chapter III is presented, along with a number of illustrative second- and third-order examples. Extensions to systems with saturation and other non-linearities are discussed in Chapter V. Finally, the results are summarized in Chapter VI.

II. CLASSIFICATION OF THE MOTIONS OF RELAY-CONTROL SYSTEMS

1. DEFINITIONS

The motions of relay-control systems were described at length by Flügge-Lotz [6] for linear switching and by Maltz [7] and Alimov [8], among others, for wider classes of switching functions; we shall follow Alimov's more mathematical treatment in most of our development.

The relay-control system is assumed to consist in general of a non-linear time invariant plant (containing only continuous elements without time delay) controlled through a single ideal relay, the system so constructed that the switching function is continuous in time. The input is assumed to be zero. This system can be described by an autonomous vector differential equation of the form

$$\dot{\underline{x}} = \underline{F}(\underline{x}) + \underline{c}(\underline{x})\,\mathrm{sgn}[\sigma(\underline{x})] \quad (2\text{-}1)$$

where

$\underline{x}$ is an n-dimensional state vector.

$\underline{F}(\underline{x})$, $c(\underline{x})$ are continuous non-linear vector-valued functions of $\underline{x}$ with continuous partial derivates; $\underline{F}(\underline{0}) = 0$.

$\sigma(\underline{x})$ is a continuous scalar function of $\underline{x}$, the switching function, with $\sigma(\underline{x}) = 0$ defining the switching surface.

$\mathrm{sgn}(\sigma)$ is the signum function of σ, to be precisely defined below.

In the examples in this work the switching function will be linear so that (2-1) becomes

$$\dot{\underline{x}} = \underline{F}(x) + \underline{c}(\underline{x})\,\mathrm{sgn}[\underline{d}^{T}\underline{x}] \quad (2\text{-}2)$$

where $\underline{d}$ is the normal to the switching hyperplane. Furthermore, in most of the examples the plant will be linear and the control magnitude

---

*Vector quantities are underlined and understood as column matrices unless otherwise indicated. The transpose is denoted by a superscript T.

a constant, $\underline{c}(\underline{x}) = \underline{b}$. The differential equation becomes

$$\dot{\underline{x}} = A\underline{x} + \underline{b}\ \mathrm{sgn}\ [\underline{d}^T\underline{x}] \tag{2-3}$$

where A is an $n \times n$ matrix of constant coefficients and $\underline{b}$ is a constant vector of n dimensions. In addition, the state vector will be represented in phase coordinates (although this is not required), in which $x_{i+1} = \dot{x}_i$, $i = 1,2,\ldots,n-1$. The differential equation then takes on the following special form

$$\begin{bmatrix} \dot{x}_1 \\ \dot{x}_2 \\ \cdot \\ \cdot \\ \cdot \\ \dot{x}_{n-1} \\ \dot{x}_n \end{bmatrix} = \begin{bmatrix} 0 & 1 & 0 & \cdot & \cdot & \cdot & \cdot & \cdot & \cdot & \cdot \\ 0 & 0 & 1 & 0 & \cdot & \cdot & \cdot & \cdot & \cdot & \cdot \\ \cdot & \cdot & & \cdot & & & & & & \\ \cdot & \cdot & & & \cdot & & & & & \\ \cdot & \cdot & & & & \cdot & & & & \\ \cdot & \cdot & & & & & \cdot & & & \\ 0 & \cdot & \cdot & \cdot & \cdot & \cdot & \cdot & \cdot & 0 & 1 \\ -a_1 & -a_2 & \cdot & \cdot & \cdot & \cdot & \cdot & \cdot & \cdot & -a_n \end{bmatrix} \begin{bmatrix} x_1 \\ x_2 \\ \cdot \\ \cdot \\ \cdot \\ x_{n-1} \\ x_n \end{bmatrix} + \begin{bmatrix} 0 \\ 0 \\ \cdot \\ \cdot \\ \cdot \\ 0 \\ -1 \end{bmatrix} \mathrm{sgn}[\underline{d}^T\underline{x}] \tag{2-4}$$

The system block diagram is shown in Figure 2-1.

The block-diagram representation of the system of Equation (2-3) consists of a transfer function with feedback around it through a relay; this characterization may also be viewed as an alternative, basic definition of the system. A thorough discussion of the connection between the black-box, transfer-function model and the differential equation characterization may be found in Reference [17]. It can be shown that the transfer function corresponding to (2-3) is given by

$$\underline{d}^T(sI - A)^{-1}\,\underline{b} \quad .$$

Equation (2-4) is just one of a variety of possible forms this representation can take; the switching function has been taken in this case to be a linear combination of all of the state variables. Another basic form corresponds to identifying σ with a single state variable (x_1) , with

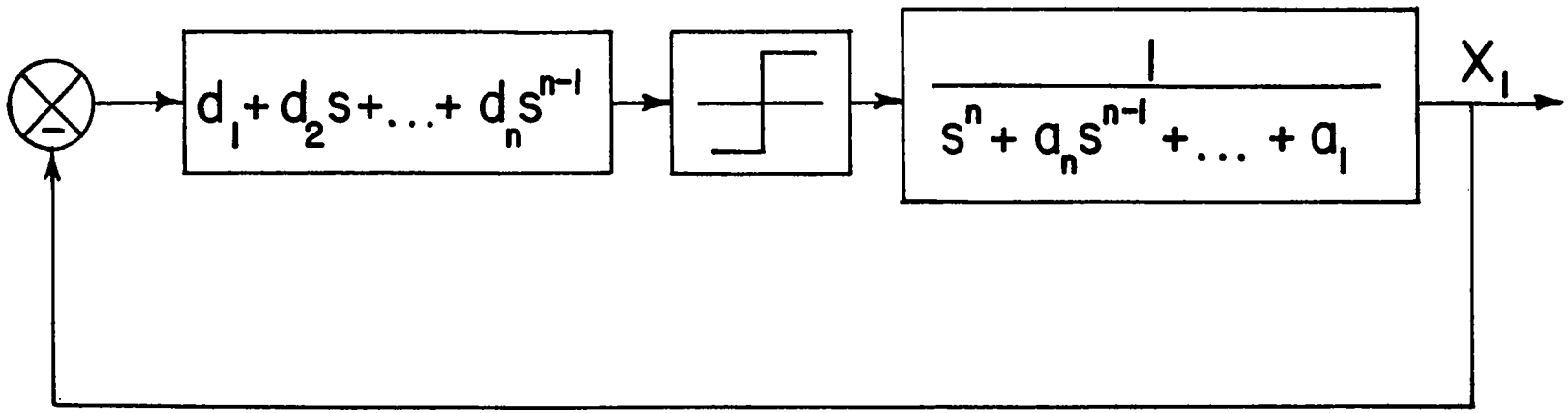

Fig. 2-1 Block Diagram of the Relay-Control System with Linear Plant and Switching.

$$A = \begin{bmatrix} 0 & 0 & 0 & . & . & 0 & -a_1 \\ 1 & 0 & 0 & . & . & 0 & . \\ 0 & 1 & 0 & . & . & . & . \\ . & 0 & . & . & . & . & . \\ . & . & . & . & . & . & . \\ . & . & . & . & . & 0 & -a_{n-1} \\ 0 & 0 & . & . & 0 & 1 & -a_n \end{bmatrix}$$

$$\underline{b} = \begin{bmatrix} d_1 \\ d_2 \\ . \\ . \\ . \\ . \\ d_n \end{bmatrix} \quad , \quad \text{and} \quad \underline{d} = \begin{bmatrix} 0 \\ 0 \\ . \\ . \\ . \\ 0 \\ -1 \end{bmatrix}$$

It is clear from the fact that the preceding formulas contain $2n$ arbitrary constants $(a_1, \ldots, a_n ; d_1, \ldots, d_n)$ that the existence of zeros in the transfer function between the relay and the system output has no bearing on the characterizations discussed above.

The signum function is the mathematical representation of an ideal relay, which we define as

$$\text{sgn}(\sigma) = \begin{cases} +1 , & \sigma > 0 \\ \varphi , & \sigma = 0 \\ -1 , & \sigma < 0 \end{cases} \qquad -1 \leq \varphi \leq 1 \qquad (2\text{-}5)$$

This definition is equivalent to that commonly employed in the representation of Coulomb friction (see, for example, Andronow and Chaikin [9]

p. 108). It can be viewed as the limiting set of points approached by the set of points on the saturation function defined by

$$\text{sat}(\sigma) = \begin{cases} +1 , & \sigma > 1/k \\ k\sigma , & |\sigma| \leq 1/k \\ -1 , & \sigma < -1/k \end{cases} \tag{2-6}$$

as $k \to \infty$ and thus is an intuitively proper choice. Most importantly, this definition simplifies the description of the motions of (2-1) on $\sigma = 0$; a particular advantage is that it creates a well-defined equilibrium at $\underline{x} = 0$.

2. MOTIONS

Solutions of (2-1) will clearly be well defined everywhere except in the neighborhood of $\sigma = 0$, where their behavior may be investigated by deriving the equation of motion in terms of σ . Form the total time derivative of σ in terms of the switching surface gradient, a row vector

$$\nabla\sigma = \left[\frac{\partial\sigma}{\partial x_1} , \frac{\partial\sigma}{\partial x_2} , \cdots, \frac{\partial\sigma}{\partial x_n} \right] ,$$

to obtain

$$\dot{\sigma} = (\nabla\sigma)\dot{\underline{x}} = (\nabla\sigma)\underline{F}(\underline{x}) + (\nabla\sigma)\underline{c}(\underline{x})\ \text{sgn}\ (\sigma) \tag{2-7}$$

For values of $\underline{x}$ satisfying the inequality

$$|(\nabla\sigma)\underline{F}| > |(\nabla\sigma)\underline{c}| \tag{2-8}$$

$\dot{\sigma}$ has the same sign on both sides of the switching surface so that a trajectory intersecting the switching surface from σ positive (negative) may be continued into the region σ negative (positive). In terms of the signum characteristic, the "fan" of possible tangent vectors (2-5) of the trajectory at the switching surface lies wholly on the new side of the surface; thus any value of φ in Equation (2-5) at switching carries the state point across the surface. (See Figure 2-2). In order to insure the uniqueness for $\dot{\underline{x}}$ for this motion, which we call regular

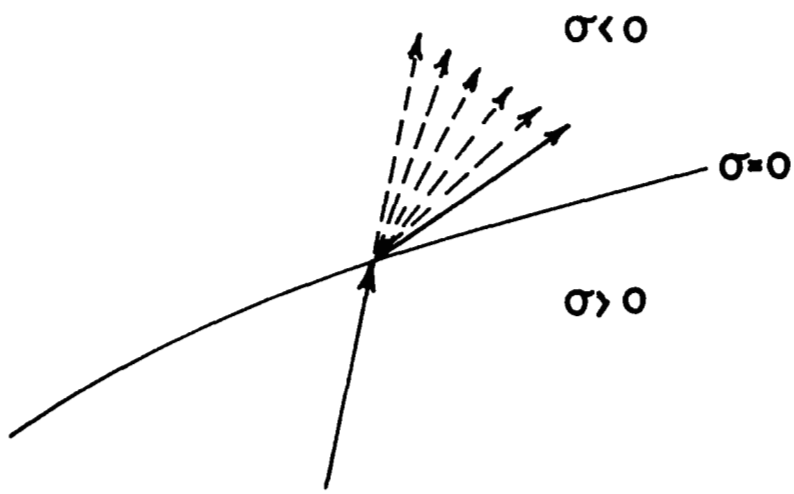

Fig. 2-2 Trajectory Directions at $\sigma = 0$ for Regular Switching.

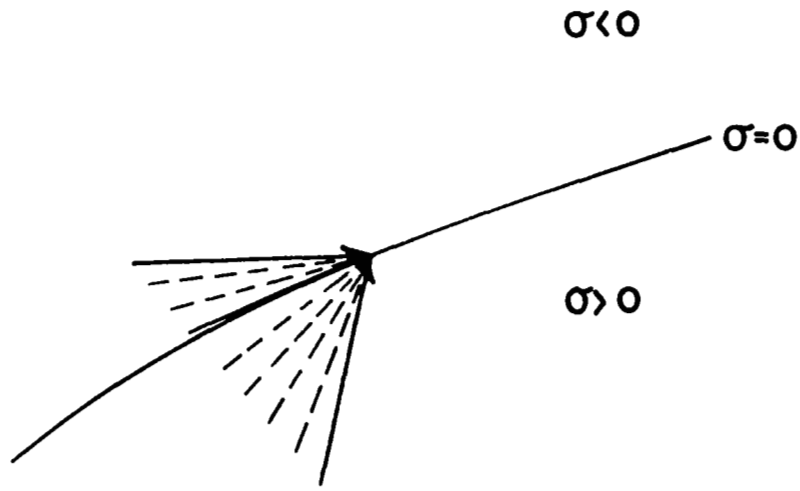

Fig. 2-3 Trajectory Directions at $\sigma = 0$ for Sliding.

switching, we arbitrarily define φ at $\sigma = 0$ under (2-8) to be $+1$. (As a consequence of definition (2-5), the particular value assumed by φ for regular switching on $\sigma = 0$ is entirely arbitrary; we fix it at $+1$ only to make the solution to (2-1) formally unique.)

For those values of $\underline{x}$ which satisfy the relations

$$|(\nabla\sigma)\underline{F}| < |(\nabla\sigma)\underline{c}| \tag{2-9}$$

or

$$|\underline{d}^T A\underline{x}| < |\underline{d}^T\underline{b}| \quad \text{for the system described by (2-3)} \tag{2-9a}$$

and

$$(\nabla\sigma)\underline{c} < 0 \tag{2-10}$$

or

$$\underline{d}^T\underline{b} < 0 \quad \text{for the system described by (2-3)} \tag{2-10a}$$

$\dot{\sigma}$, from (2-7), is opposite in sign to σ and independent of its magnitude; thus motions in the neighborhood of the switching surface are driven to the surface and forced to remain there once the surface is reached, for as long as (2-9) and (2-10) hold. The orientation of the fan of tangent directions on the switching surface in Figure 2-3 shows that only one of these tangent directions is allowable, corresponding to a unique value of φ. This constrained motion is known as chatter in western literature. The name derives from the observed behavior of a physical relay operating in this mode. Due to small time delays in switching, the state point does not remain precisely on the switching surface; rather it "chatters" with a small amplitude at a high frequency from side to side of the switching surface. On the average for small time delays the state point for the physical relay proceeds on the switching surface and approximates the mathematical idealization proposed here. In Soviet literature this motion is referred to as sliding; this terminology seems more in keeping with our idealization, since the preceding results indeed imply that the state point "slides" on the switching surface. The term "sliding" will therefore be used exclusively here to clarify the distinction between ideal "sliding" and physical

"chattering" with its high frequency components of motion. It should be kept in mind, however, that the behavior of a sliding system closely approximates a chattering one for sufficiently small relay imperfections.

The output of the relay, φ, for a sliding trajectory may be determined by setting $\text{sgn}(\sigma) = \varphi$ and $\dot{\sigma} = 0$ in (2-7) and solving for φ. The result is

$$\varphi = \frac{-(\nabla\sigma)\underline{F}}{(\nabla\sigma)\underline{c}} \tag{2-11}$$

The equation of motion for sliding may be expressed in first-order form by substituting the expression for φ from (2-11) for $\text{sgn}(\sigma)$ in (2-1):

$$\dot{\underline{x}} = \underline{F} - \underline{c}(\nabla\sigma)\underline{F}/(\nabla\sigma)\underline{c} \tag{2-12}$$

or

$$\dot{\underline{x}} = \left[I - \frac{\underline{c}(\nabla\sigma)}{(\nabla\sigma)\underline{c}} \right] \underline{F} = \hat{\underline{F}}(\underline{x}) \tag{2-13}$$

on

$$\sigma(\underline{x}) = 0$$

For (2-3), the equation is a linear one

$$\dot{\underline{x}} = \left[I - \frac{\underline{b}\underline{d}^T}{\underline{d}^T\underline{b}} \right] A\underline{x} = \hat{A}\underline{x} \tag{2-13a}$$

on

$$\underline{d}^T\underline{x} = 0 \ *$$

If phase coordinates (2-4) are used, sliding motions are described simply by the (n-1)st-order differential equation in x_1,

$$\sigma(x_1) = \sigma[x_1, \dot{x}_1, \ \ldots, \ x_1^{(n-1)}] = 0 \tag{2-14}$$

---

*$\sigma(\underline{x}) =$ constant and $\underline{d}^T\underline{x} =$ constant are solutions to (2-13) and (2-13a), respectively, since these equations were derived from the condition $\dot{\sigma} = 0$ [eq. (2-7)]; the auxiliary conditions $\sigma(\underline{x}) = 0$ and $\underline{d}^T\underline{x} = 0$ are thus necessary to properly constrain the solution to the switching surface.

(The continuity condition on σ requires that it contains at most the (n-1)st derivative of x_1.)

Another characteristic of solutions on $\sigma = 0$ will be mentioned for completeness. If, in addition to (2-9) and in place of (2-10),

$$(\nabla\sigma)\underline{c} > 0 \qquad (2\text{-}15)$$

then trajectories intersecting the switching surface all leave the surface; points on the switching surface where this condition holds have been named "starting points" [6], since trajectories may originate at these points but never arrive there. Conditions leading to the existence of starting points are usually avoided in the design of relay-control systems and thus are normally of no practical interest; starting points will therefore be ignored here.

If both $(\nabla\sigma)\underline{F}$ and $(\nabla\sigma)\underline{b}$ are zero, then $\dot{\sigma}$ is also zero from (2-7) and $\ddot{\sigma}$ must be examined in order to determine the motion in the neighborhood of $\sigma = 0$. This case will also not be considered here; conditions analogous to (2-9) and (2-10) for a sliding motion are given by Alimov [8].

In conclusion, the motions of (2-1) based on (2-5) may be summarized as follows: Solutions exist everywhere, and if $(\nabla\sigma)\underline{c} \leq 0$ (no starting points), trajectories proceed in a well-defined direction at each point in the state space.

III. LYAPUNOV'S DIRECT METHOD

1. THE MAIN THEOREM

The idea of the Direct Method is well known and discussed in detail in a number of references [1], [2], [3], so that only the essential results will be presented here.

Consider an ordinary differential equation with a single equilibrium at $\underline{x} = 0$.

$$\dot{\underline{x}} = \underline{\mathfrak{F}}(\underline{x}) \ , \ \underline{\mathfrak{F}}(\underline{0}) = \underline{0} \tag{3-1}$$

Let $\underline{\mathfrak{F}}$ be sufficiently well behaved that solutions of (3-1) (given by $\underline{\psi}(\underline{x}^o, t)$ with initial state $\underline{x}^o$ and initial time taken as zero) exist everywhere.

The following theorem (see Hahn[1] and LaSalle[2]) gives sufficient conditions for the determination of a subdomain of the domain of asymptotic stability of (3-1), which we will call simply the estimate of the stability domain*:

Theorem 1 The equilibrium of (3-1), $\underline{x} = \underline{0}$, is asymptotically stable (A. S.) in a domain R if there can be found a continuous scalar function V (to be called a Lyapunov function) such that

(1) $V(\underline{x})$ is positive definite in R .

(2) $V(\underline{x})$ = constant is a closed surface bounding R .

(3) $\dot{V}(\underline{x})$ is negative semi-definite in R .

(4) $\dot{V}(\underline{x})$ does not vanish identically on a trajectory of (3-1) in R .

$\dot{V}(\underline{\xi})$ is the time rate of change of V evaluated on a trajectory of (3-1)

$$\dot{V}(\underline{\xi}) = \lim_{\Delta \to 0} \frac{V[\underline{\psi}(\underline{\xi},\Delta)] - V[\underline{\psi}(\underline{\xi},0)]}{\Delta} \tag{3-2}$$

---

* The equilibrium $\underline{x} = \underline{0}$ is said to be asymptotically stable in a domain R if

i.) For every ϵ there exists a δ such that if $\|\underline{x}^o\| < \delta$ then $\|\underline{\psi}(\underline{x}^o,t)\| < \epsilon$ for all $t > 0$

ii.) $\lim_{t \to \infty} \underline{\psi}(\underline{x}^o,t) = \underline{0}$ for all $\underline{x}^o$ in R .

The surface with the greatest value of V = constant = C_{max} which satisfies the conditions of Theorem 1 gives the boundary of the largest stability-domain estimate. In Figure 3-1 this surface is the one just tangent to the surface $\dot{V} = 0$ and thus has the largest value of V of those surfaces lying wholly within the space $\dot{V} \leq 0$. The determination of this boundary in practice is a difficult matter in all but the very simplest cases. The numerical techniques developed and used in Reference [4] for determining stability boundaries for second- and third-order systems have been used in this work in the testing of the V functions described below to determine stability boundaries for relay-control systems.

2. APPLICATION OF A SPECIAL LYAPUNOV FUNCTION TO RELAY-CONTROL SYSTEMS

Consider as a candidate for a Lyapunov function for (2-3) a function of the Lur'e form (a symmetric quadratic form plus the integral of the nonlinearity)

$$V = \frac{1}{2}\underline{x}^T H\underline{x} + \int_0^{\sigma} \text{sgn}(\sigma)d\sigma$$

$$V = \frac{1}{2}\underline{x}^T H\underline{x} + \underline{d}^T\underline{x}\ \text{sgn}\ (\underline{d}^T\underline{x}) \qquad (3\text{-}3)$$

(It will be shown that (3-3) is also a suitable function for (2-2).) The time rate of change of V, $\dot{V}$, on trajectories of (2-2) must be evaluated differently depending on whether or not the trajectory is constrained to lie on the switching surface in a sliding motion. For regular switching

$$\text{sgn}\ (\sigma) = \pm 1 \qquad (3\text{-}4)$$

$\dot{V}$ is given simply by

$$\dot{V} = (\underline{\nabla} V)\dot{\underline{x}} \qquad (3\text{-}5)$$

In accordance with the convention established in Chapter II, that $\text{sgn}(\sigma) = +1$ in (2-2) on $\sigma = 0$ for regular switching, we also define $\text{sgn}(\sigma)$ in (3-3) to be positive for $\sigma = 0$. Thus (3-5) is unambiguous and can readily be evaluated from (3-3) and (2-2) to be

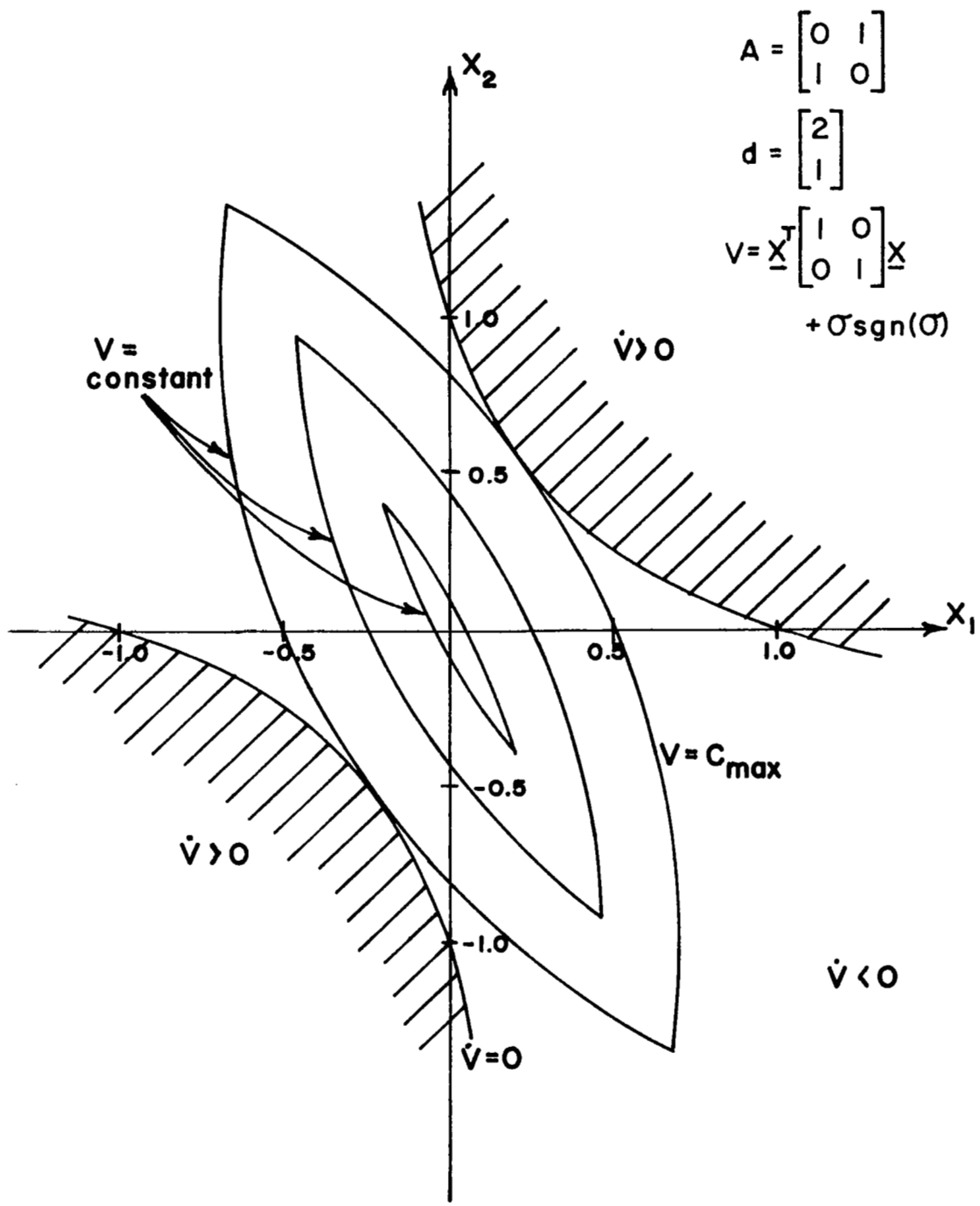

Fig. 3-1 Stability Boundary Determined from a Lyapunov Function

$$\dot{V} = \frac{1}{2}\left[\underline{F}(\underline{x})^T H\underline{x} + \underline{x}^T H\underline{F}(\underline{x})\right] + \left[\underline{c}(\underline{x})^T H\underline{x} + \underline{d}^T\underline{F}(\underline{x})\right]\mathrm{sgn}(\sigma) + \underline{d}^T\underline{c}(\underline{x}) \qquad (3\text{-}6)$$

If $\underline{F}(\underline{x})$ and $\underline{c}(\underline{x})$ are expanded in Taylor series

$$\underline{F}(\underline{x}) = A\underline{x} + \underline{O}(\underline{x}^2)^* \qquad (3\text{-}7)$$

and

$$\underline{c}(\underline{x}) = \underline{b} + C\underline{x} + \underline{O}(\underline{x}^2) \qquad (3\text{-}8)$$

The constant term of the expansion (3-7) has been set equal to zero because there is an equilibrium of (2-2) at $\underline{x} = \underline{0}$. $\dot{V}$ can then be written

$$\dot{V} = \frac{1}{2}\underline{x}^T Q\underline{x} + \underline{k}^T\underline{x}\ \mathrm{sgn}\ \sigma + \underline{d}^T\underline{b} + O(\underline{x}^3) + O(\underline{x}^2)\mathrm{sgn}\ \sigma + O(\underline{x}) \qquad (3\text{-}9)$$

where

$$Q = A^T H + HA$$

and

$$\underline{k} = H\underline{b} + A^T\underline{d}$$

For the linear plant and constant control magnitude case of (2-3) this equation simplifies to

$$\dot{V} = \frac{1}{2}\underline{x}^T Q\underline{x} + \underline{k}^T\underline{x}\ \mathrm{sgn}\ \sigma + \underline{d}^T\underline{b} \qquad (3\text{-}9a)$$

For sliding, since $\sigma = 0$, the Lyapunov function assumes the simpler form

$$V_s = \frac{1}{2}\underline{x}^T H\underline{x} \qquad (3\text{-}10)$$

(The subscript s denotes quantities evaluated on a sliding trajectory.)

---

* $\underline{O}(\underline{x}^n)$ denotes vector-valued functions of $\underline{x}$ whose components are $O(\underline{x}^n)$, terms of at least n th order in the x_i.

Using (3-10), the sliding mode velocity given by (2-13), and the series expansion

$$\hat{\underline{F}}(\underline{x}) = \hat{A}\underline{x} + \underline{O}(\underline{x}^2) \tag{3-11}$$

the time rate of change of V in sliding is

$$\dot{V}_s = \frac{1}{2}\left[\hat{\underline{F}}(\underline{x})^T H\underline{x} + \underline{x}^T H\hat{\underline{F}}(\underline{x})\right] \tag{3-12}$$

or

$$\dot{V}_s = \frac{1}{2}\underline{x}^T\hat{Q}\underline{x} + O(\underline{x}^3) \tag{3-13}$$

where

$$\hat{Q} = \hat{A}^T H + H\hat{A}$$

For the system of (2-3), equation (3-13) simplifies to

$$\dot{V}_s = \frac{1}{2}\underline{x}^T\hat{Q}\underline{x} \tag{3-13a}$$

The application of these results will be illustrated with several simple examples.

Example 3-1.

Consider the system represented by the block diagram of Figure 3-2 and the differential equation*

$$\begin{bmatrix}\dot{x}_1\\ \dot{x}_2\end{bmatrix} = \begin{bmatrix}0 & 1\\ 1 & 0\end{bmatrix}\begin{bmatrix}x_1\\ x_2\end{bmatrix} + \begin{bmatrix}0\\ -1\end{bmatrix}\operatorname{sgn}(2x_1 + x_2) \tag{3-14}$$

Take as a possible Lyapunov function

$$V = \frac{1}{2}\underline{x}^T\begin{bmatrix}1 & 0\\ 0 & 1\end{bmatrix}\underline{x} + (2x_1 + x_2)\operatorname{sgn}(2x_1 + x_2) \tag{3-15}$$

* The uncontrolled system is unstable, with roots at $+1$ and -1.

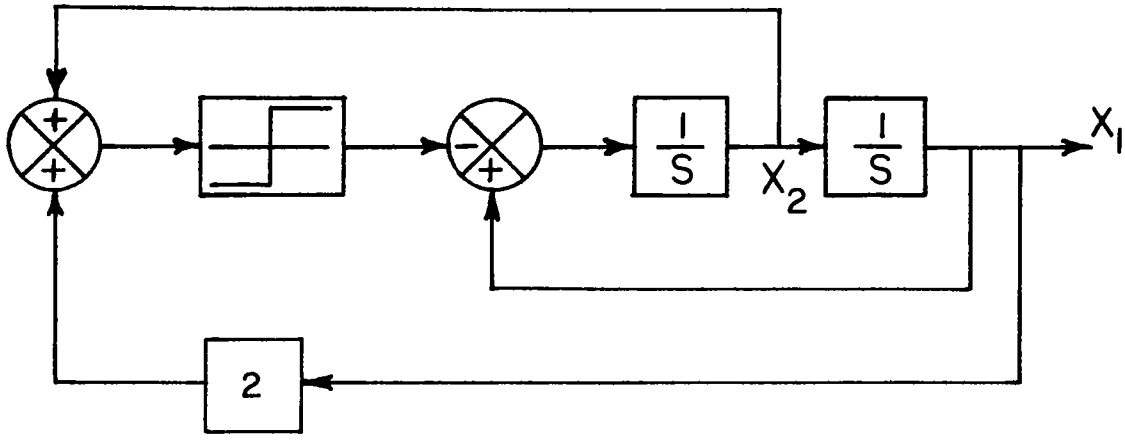

Fig. 3-2 The System of Example 3-1.

$\dot{V}$ may be evaluated for $\sigma \neq 0$ according to (3-9) as

$$\dot{V} = 2x_1x_2 + (x_1 + x_2)\text{sgn}(2x_1 + x_2) - 1 \tag{3-16}$$

Figure 3-1 shows the regions of positive and negative $\dot{V}$ in the plane and a plot of the curve $V = C_{max}$.

From (2-9a) and (2-10a) sliding will occur on $2x_1+x_2 = 0$ for

$$|x_1 + 2x_2| < 1 \tag{3-17}$$

Thus sliding occurs for $(2/3) > x_2 > -(2/3)$. The sliding equation is, from (2-13a),

$$\dot{\underline{x}} = \begin{bmatrix} 0 & 1 \\ 0 & -2 \end{bmatrix} \underline{x} = \hat{A}\underline{x} \tag{3-18}$$

($\hat{A}$ can also be easily obtained by noting that $\dot{x}_1$ remains equal to x_2 and that on the switching line $x_2 = -2x_1$ or $\dot{x}_2 = -2\dot{x}_1 = -2x_2$.)

$$V_s = \frac{1}{2} x_1^2 + \frac{1}{2} x_2^2 \tag{3-19}$$

$\dot{V}_s$ can be evaluated by differentiating (3-19) according to (3-18):

$$\dot{V}_s = x_1\dot{x}_1 + x_2\dot{x}_1 = x_1x_2 - 2x_2^2 = -4x_2^2 \tag{3-20}$$

which is clearly negative definite on $x_1 = -2x_2$. The region in Figure 3-1 bounded by $V = C_{max}$ is therefore an estimate of the stability domain since we have demonstrated that $\dot{V}$ is negative definite on all trajectories.*

Example 3-2.

Consider the same basic system with a different switching function:

$$\underline{d}^T\underline{x} = x_2 - x_1 \tag{3-21}$$

Take for a Lyapunov function the same form

* The true stability domain for this system is shown later in Figure 4-2.

$$V = \frac{1}{2} x_1^2 + \frac{1}{2} x_2^2 + (x_2 - x_1)\mathrm{sgn}(x_2 - x_1) \tag{3-22}$$

Then

$$\dot{V} = 2x_1x_2 + (x_1 - 2x_2)\mathrm{sgn}(x_2 - x_1) - 1 \tag{3-23}$$

for regular switching. Regions of positive and negative $\dot{V}$ are shown in Figure 3-3 together with a plot of the curve $V = C_{max}$. In this example the boundary between regions of positive and negative $\dot{V}$ does not everywhere consist of curves $\dot{V} = 0$ since $\dot{V}$ changes sign discontinuously across this boundary when it coincides with $\sigma = 0$. Sliding still occurs for this system (since again $\underline{d}^T\underline{b} < 0$), the region being given by (2-9a) as

$$|- x_1 + x_2| < 1 \tag{3-24}$$

the whole switching line. $\hat{A}$ may be computed as before.

$$\hat{A} = \begin{bmatrix} 0 & 1 \\ 0 & 1 \end{bmatrix} \tag{3-25}$$

$\dot{V}_s$, evaluated by differentiating (3-19) according to (3-25), is

$$\dot{V}_s = x_1\dot{x}_1 + x_2\dot{x}_2 = x_1x_2 + x_2^2 = 2x_2^2 \tag{3-26}$$

which is positive definite along the entire line $x_1 = x_2$. Thus Theorem 1 is not satisfied for any value of V = constant and the stability domain estimate is not valid.

This example illustrates the necessity of including sliding effects in a Lyapunov function analysis, since the partial analysis of this example implied stability, while the equilibrium is clearly unstable because sliding trajectories proceed away from the origin.

These examples also suggest the following assertion: The existence of a stability domain is determined by the stability of the sliding motion in the neighborhood of the equilibrium, when sliding is present. This may be readily demonstrated as follows: If sliding exists, $\underline{d}^T\underline{b}$

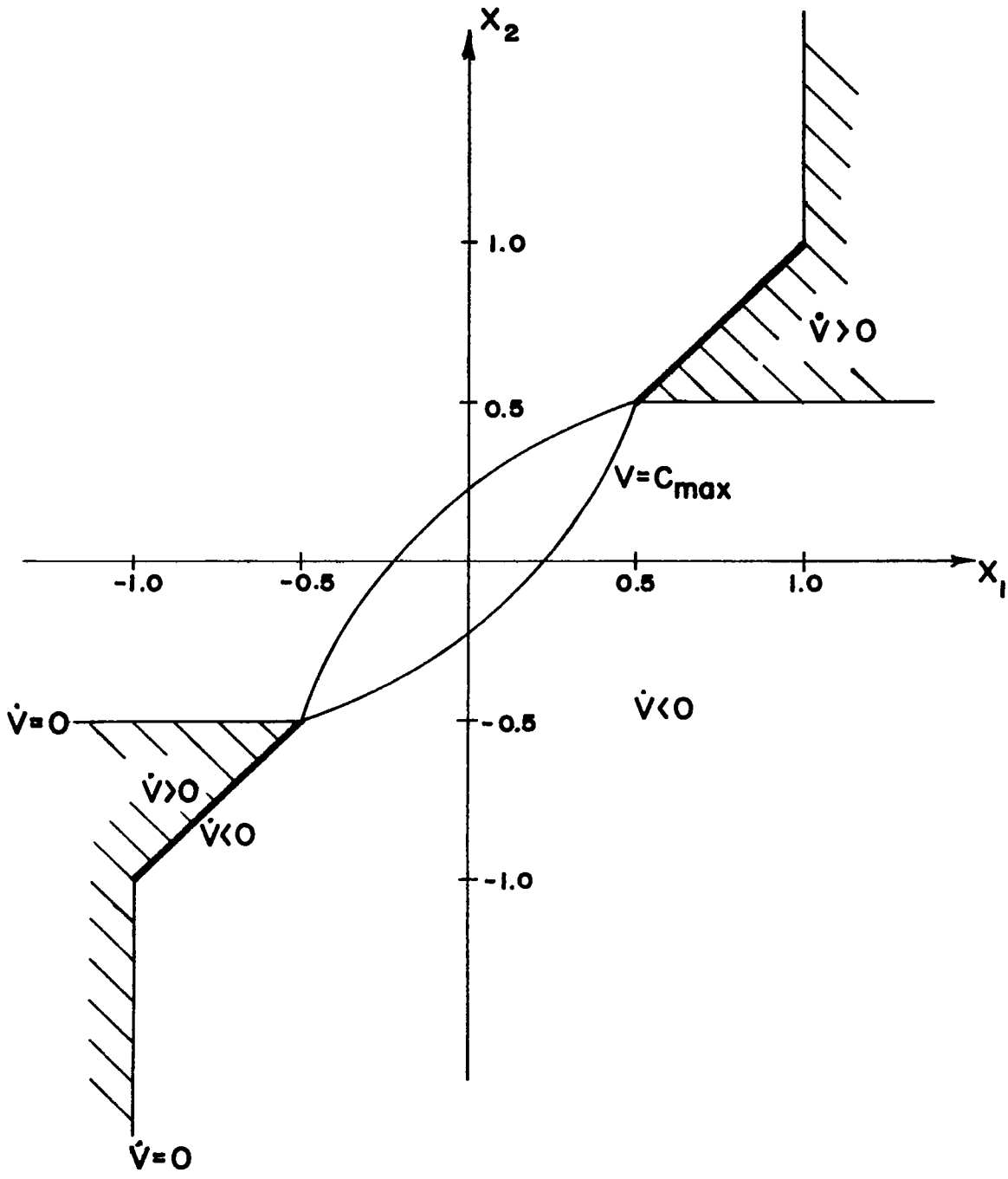

Fig. 3-3 Stability Boundary for Example 3-2.

is a negative number and thus we can find a neighborhood of $\underline{x} = \underline{0}$, $\|\underline{x}\| < \epsilon$ with ϵ sufficiently small, in which $\dot{V}$ in (3-9) is everywhere negative, for any H. Thus any positive definite V of the form (3-3) will be a Lyapunov function for regular switching. Consider now $\dot{\underline{x}}$ and V for sliding:

$$\dot{\underline{x}}_s = \hat{A}\underline{x} + \underline{0}(\underline{x}^2) \tag{3-27}$$

$$V_s = \frac{1}{2}\underline{x}^T H \underline{x} \tag{3-28}$$

Let R be an orthogonal transformation from $\underline{x}$ to $\underline{y}$ such that y_n is normal to the switching plane.* Then

$$\dot{\underline{y}}_s = R\hat{A}R^T\underline{y} + \underline{0}(\underline{y}^2) \tag{3-29}$$

and

$$V_s = \frac{1}{2}\underline{y}^T RHR^T \underline{y} \tag{3-30}$$

where use is made of the fact that the inverse of an orthogonal matrix is equal to its transpose. $\dot{y}_n = 0$ in sliding. Therefore the y_n coordinate may be neglected and new $n-1$ st.-order equations in $\underline{z} = [y_1, y_2, \ldots, y_{n-1}]^T$ written:

$$\dot{\underline{z}}_s = A'\underline{z} + \underline{0}(\underline{z}^2) \tag{3-31}$$

and

$$V_s = \frac{1}{2}\underline{z}^T H' \underline{z} \tag{3-32}$$

where $A' = R\hat{A}R^T$ and $H' = RHR^T$ with the n th columns and rows deleted. If sliding is stable the eigenvalues of A' must have negative real parts, and thus by a well known result [1] it is always possible to find a set of positive definite H' matrices that make

*An example of such a transformation may be found in Appendix B, where it is employed in a computation of the volume within V = constant for a third-order V of the form (3-3).

$$\dot{V}_s = \frac{1}{2}\underline{z}^T(A'^T H' + H'A')\underline{z} + O(\underline{z}^3)$$

$$= \frac{1}{2}\underline{z}^T Q'\underline{z} + O(\underline{z}^3) \qquad (3\text{-}33)$$

negative definite and thus (3-32) a Lyapunov function for (3-31) in a sufficiently small neighborhood of the origin. If sliding is unstable, clearly no stability region exists since an unstable trajectory of (3-31) leads away from the origin. This discussion not only shows that the stability of sliding motions (when sliding exists) is a necessary and sufficient condition for the stability of (2-2) but also that a set of Lyapunov functions (3-3) always exists to estimate the stability domain of (2-2) when a sliding mode is present. (Note that in the second-order case it is actually not necessary to check $\dot{V}_s$ since if sliding is stable, $\dot{V}_s < 0$ for any positive definite V.)

Complete conditions for A.S. of the equilibrium of (2-3) in the form (2-4) may be found in Anosov [10]. Interpreted in terms of the root locus based on Figure 2-1 with a gain K in place of the relay, a single necessary and sufficient condition is that the locus of all roots lie in the left half plane in the limit as $K \to \infty$.

IV. METHODS OF GENERATING LYAPUNOV FUNCTIONS

1. EXISTING METHODS

Since in general an infinite number of Lyapunov functions exist for a particular system, the problem of finding some Lyapunov function is not difficult. However, the problem of finding one which gives a useful approximation to the stability domain is a formidable one and a task to which a number of workers have devoted their attentions, among them Zubov[5], Ingwerson [11,12] , Schultz and Gibson[13], and Szegö[14].

The Zubov technique consists of finding approximate power series solutions, V , to the partial differential equation

$$\dot{V} = [\nabla V(\underline{x})]\mathfrak{F}(\underline{x}) = - \theta(\underline{x})[1 - V(\underline{x})] \qquad (4\text{-}1)$$

where $\mathfrak{F}(\underline{x})$ (see equation (3-1)) has a power series expansion in $\underline{x}$ about $\underline{0}$ and $\theta(\underline{x})$ is positive semi-definite. The requirements on $\mathfrak{F}(\underline{x})$ exclude discontinuous systems A further disadvantage of this method is that the convergence of the series solution is not uniform and may be quite slow and erratic [4]. The speed of convergence is very sensitive to the choice of θ , which unfortunately must be based on experience.

The most systematic method among the others is Ingwerson's in which the Jacobian of $\underline{\mathfrak{F}}$ is used, in analogy with the linear case, to form a matrix of second partial derivatives of a scalar function which may be integrated twice to form V . Although the method is not guaranteed to work, the results are quite often good. Like Zubov, however, a critical decision is involved in choosing a form for $\dot{V}$; in fact the quantity chosen is the same in both cases: The quadratic or lowest-order terms of $\dot{V}$. Again, in Ingwerson's method success is dependent on a good choice of these terms, which depends, apparently, on a combination of perseverance and again skill gained through experience.

Unlike Zubov's method, Ingwerson's is applicable to discontinuous systems. However, a restriction imposed by his special integrating procedure prevents the non-linear terms of $\underline{\mathfrak{F}}(\underline{x})$ from appearing in the

Lyapunov function with more than two different state variables as arguments. In the relay-control case this means that the switching surface cannot be made the locus of discontinuities in $\underline{\nabla} V$ for systems of third order (containing all three state variables in the switching function) or higher. Since in general the surfaces bounding true stability domains have this locus of discontinuities in their gradients, this restriction limits the scope of the method.

The techniques of Schultz and Gibson and Szegö are less systematic than that of Ingwerson and amount to policies rather than algorithms; these approaches gain in flexibility by requiring more choice, skill, and industry of the user. In general, they suffer from a defect in common with Ingwerson's; all attempt to incorporate the system's nonlinearities into a valid Lyapunov function in hope that the resulting function will happen to be a useful one. (In the case where a demonstration of global A.S. is desired, however, the search for a Lyapunov function can be made more systematic[13].) Two problems are associated with this approach: First, it is difficult to determine how good the result is without knowledge of the exact solution. Second, there is no systematic way to improve the results. In a sense, these methods are indirect. Considerable effort and ingenuity are expended on producing a Lyapunov function of more or less complex form; the goal of achieving a useful form is attained (if it is attained at all) only as a rather indirect result of the generating process. A more direct method, and one more readily applicable to relay-control systems, is the subject of the remainder of this work.

2. A METHOD BASED ON A STEEPEST-ASCENT TECHNIQUE

This method has two basic elements: (1) a class of Lyapunov functions depending on a set of parameters and (2) a digital computer to "rank" the functions and search for the "best" one in the class. In a sense it replaces the complex functions of other methods with a multiplicity of simple functions and substitutes for the user's skill and limited time the relatively unbounded industry of the digital computer.

In the majority of applications the "best" or most useful Lyapunov function is the one which produces the greatest estimate of the stability domain. A suitable figure of merit for a Lyapunov function V, then, is the hypervolume (called simply hereafter the volume and denoted by I) contained within the estimate of the stability boundary given by $V = C_{max}$. Intuitively one feels that from among a set of Lyapunov functions of a fixed form, the function which is optimum in the sense of having the greatest volume will also produce the best stability-boundary approximation.

With a sufficiently well-defined performance measure depending on a set of adjustable parameters it is possible to use one of the well-established surface-searching techniques [15] to find the location of the optimum in parameter space. Such a procedure is made possible in this case by the use of a computer program for determining tangencies, computing volumes, and performing a numerical search.

Consider (3-3) as the form to be optimized for the relay system (2-2). The possible positive coefficient multiplying the term on the right of (3-3) was arbitrarily taken as unity to fix the scale of V; the adjustable parameters are the independent elements of the symmetric square matrix H, of which there are $n(n+1)/2$. In general, the conditions that these elements must satisfy are not very restrictive; for example, for second-order A. S. systems with a sliding mode any positive definite V of the form (3-3) is a Lyapunov function for (2-2).

The linear form of the switching function has been postulated to facilitate the computation of the volume within $V = C_{max}$, which may be performed analytically in this case; the computations for second- and third-order systems are performed in Appendix A and B. For a general non-linear switching function a numerical integration procedure would be required. Such a procedure is practical for second-order systems but becomes quite cumbersome and time consuming for third-order systems. (Several alternatives for treating non-linear switching will be mentioned later.)

From among many existing surface-searching techniques a steepest-

ascent method was selected for its simplicity of mechanization. Let the adjustable parameters be p_i , $i = 1,2,...m$. $V(\underline{x},\underline{p})$ is a Lyapunov function for the system under consideration for values of $\underline{p}$ consistent with certain constraints. (In optimization problems the optimum is often located on a constraint surface; in this problem, however, it was found that the functions on a constraint boundary ordinarily have a measure I of zero and are automatically avoided by a systematic search procedure.) At a starting point given by $\underline{p}^{(0)}$, the values of the performance index $I^{(0)}$ and its gradient $\underline{\nabla} I^{(0)} = [\partial I/\partial p_1 \ ... \ \partial I/\partial p_m]^{(0)}$ are computed and a step of some pre-determined magnitude ds_0 is taken in the direction of $\underline{\nabla} I^{(0)}$ in the $\underline{p}$ space. The location of the new point is given by

$$\underline{p}^{(1)} = \underline{p}^{(0)} + ds_0 \underline{\nabla}^T I^{(0)} \qquad (4\text{-}2)$$

If $I^{(1)} > I^{(0)}$ the new point is accepted and the process is repeated with $\underline{p}^{(1)}$ now as the starting point. If $I^{(1)} < I^{(0)}$ the step size is halved to $ds_1 = ds_0/2$ and a new point

$$\underline{p}^{(1)} = \underline{p}^{(0)} + ds_1 \underline{\nabla}^T I^{(0)}$$

is tested; this procedure is continued until either $I^{(1)} > I^{(0)}$ (in which case a new step is made at the current step size) or else the step size reaches some pre-set lower limit and the search is terminated.

Although I is evaluated analytically, the computation is cumbersome and the result is not obtained in a single, closed form. Therefore the gradient of I is computed numerically by successively perturbing the elements of $\underline{p}$.

A simplified block diagram of the entire process is shown in Figure 4-1. The block labeled "Find Tangency" contains the program described in detail in Reference[4] which performs the rather complex computations of C_{max} . Briefly, this program carries out the following operations, beginning with given V and $\mathfrak{F}$ functions and a pre-determined starting point in state space:

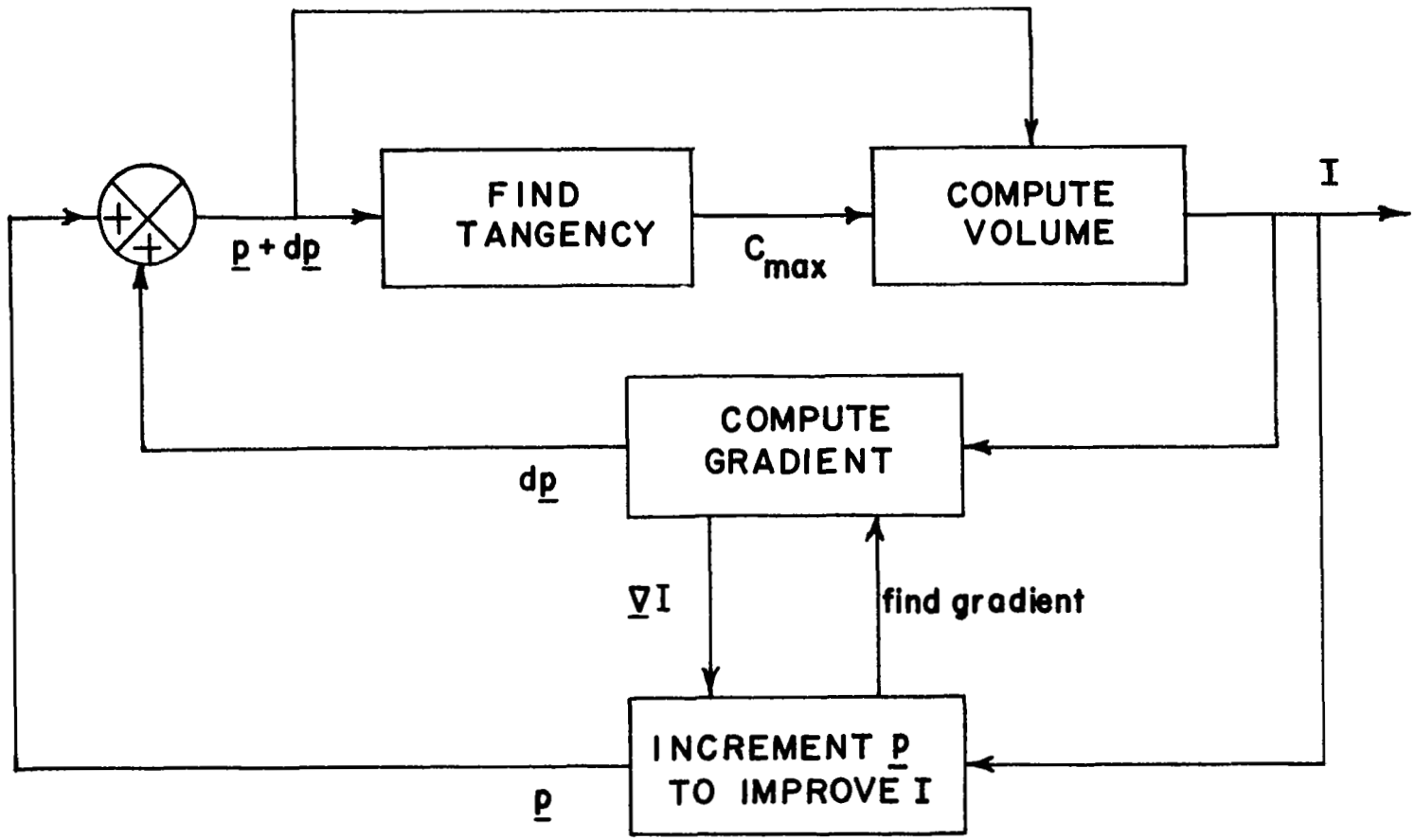

Fig. 4-1 Flow-Diagram for the Steepest-Ascent Method.
(The program is started by assuming a vector p.)

A.) A point on a surface $\dot{V} = 0$ is found by either spiralling outwards from the origin if the starting point is in a region of $\dot{V} < 0$ or, if $\dot{V}$ is initially positive, marching in steps in the direction of the negative gradient of $\dot{V}$.

B.) A minimum of V is found on the $\dot{V} = 0$ surface by a gradient search process, and this value of V is accepted tentatively as C_{max} .

C.) Optionally, the program traces out intersections of $V = C_{max}$ with selected planes in order to test the validity of the tangency. If an intersection curve passes into a region of positive $\dot{V}$, the value of C_{max} is rejected and the search is begun again for the true, global minimum of V on $\dot{V} = 0$.

Considerable time may be saved by deleting part C.) whenever possible. Thus, the tangencies found on perturbations of $\underline{p}$ were not verified by plotting, since they were nearly certain to be valid if the nominal tangency was valid itself. Detailed verification of tangencies may also be deferred to the final result with high confidence if the possible multiple local tangencies may be classified and a directed search performed for each type, with a consequent selection of the lowest value of C_{max} . This procedure was carried out in practice and will be discussed with illustrative examples.

Computation time may also be saved on perturbations by modifying the starting point to be very close to the nominal point of tangency in a region $\dot{V} > 0$, thus effectively reducing the time required to find the new, perturbed point of tangency.

More of the details of this process will be discussed in the examples which follow. The numerical calculations were performed on the IBM 7090 computer for early examples and on the Burroughs B5000 computer for later ones.

3. ILLUSTRATIVE EXAMPLES: SECOND-ORDER SYSTEMS

Second-order examples will be discussed at length first since they offer the clearest demonstration of the method.

Example 4-1

Consider the system of Example 3-1 pictured in Figure 3-2.

$$\dot{x}_1 = x_2$$

$$\dot{x}_2 = x_1 - \text{sgn}(2x_1 + x_2) \qquad (4\text{-}3)$$

To start the process H was taken initially as the identity matrix. Starting with a step size of 0.5, after eight iteration steps the computation terminated when the step size fell below the perturbation size $(.01)$, which was taken as a lower limit. The results are shown in Figure 4-2 where the initial and final "optimum" stability domain estimates are shown together with the true (open) boundary, which is approximated quite well over a large region. The true boundary was found by constructing and examining phase-plane trajectories. The computed boundary was given by $C_{max} = 1.913$. The computed optimum H was

$$H = \begin{bmatrix} -0.04 & 0.91 \\ 0.91 & 1.89 \end{bmatrix}$$

which is clearly indefinite, demonstrating that a positive definite H is not necessary to produce a V of the form (3-3) which is positive definite in a finite region.

Example 4-2

Consider the system (also treated by Ingwerson[12])*

$$\dot{x}_1 = x_2$$

$$\dot{x}_2 = -x_1 + x_2 - \text{sgn}(x_1 + x_2) \qquad (4\text{-}4)$$

represented in block-diagram form in Figure 4-3. Again H was taken

*The uncontrolled system has a pair of complex roots $+ 1/2 \pm j(\sqrt{3}/2)$.

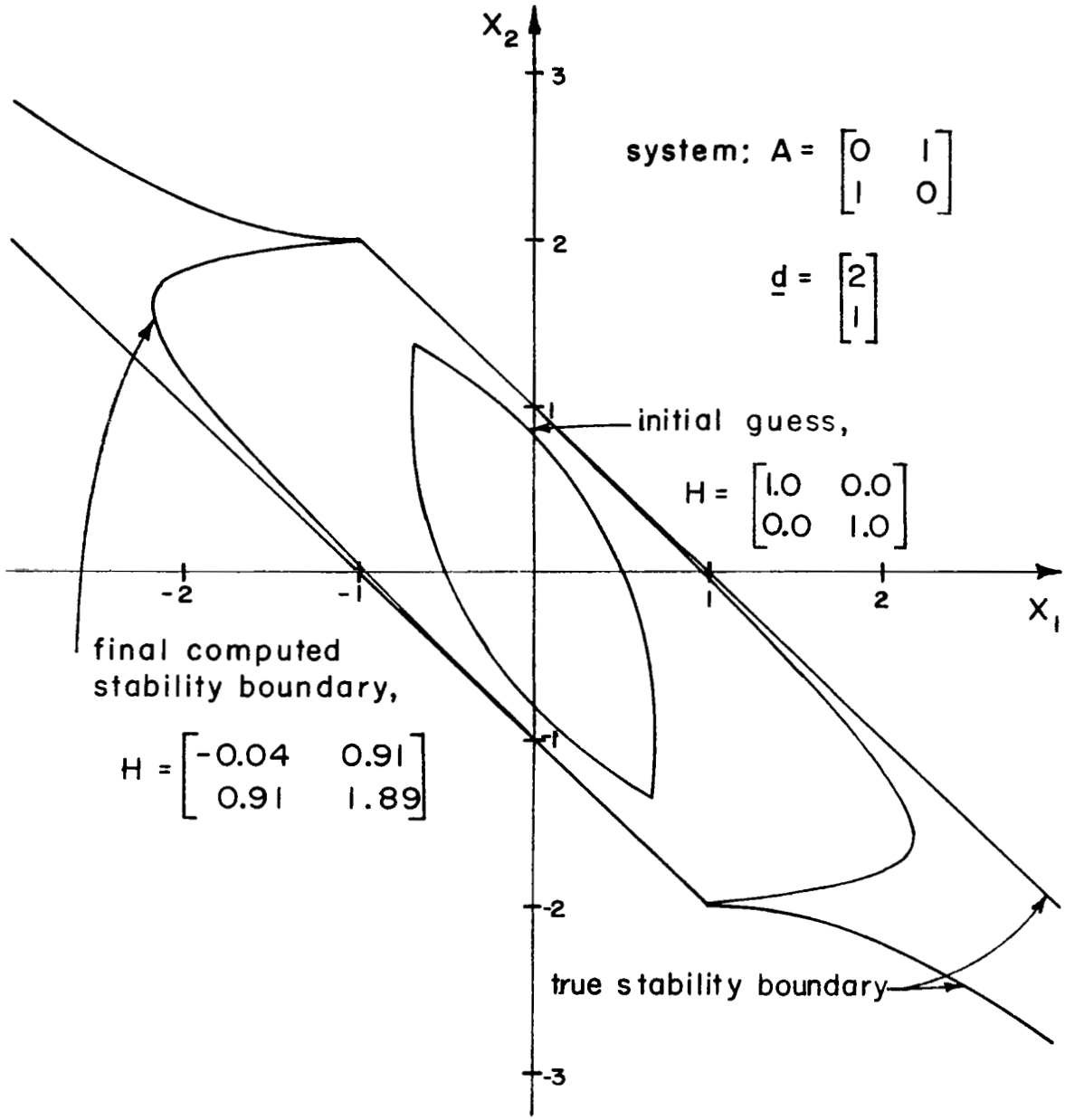

Fig. 4-2 Stability Boundaries for Example 4-1.

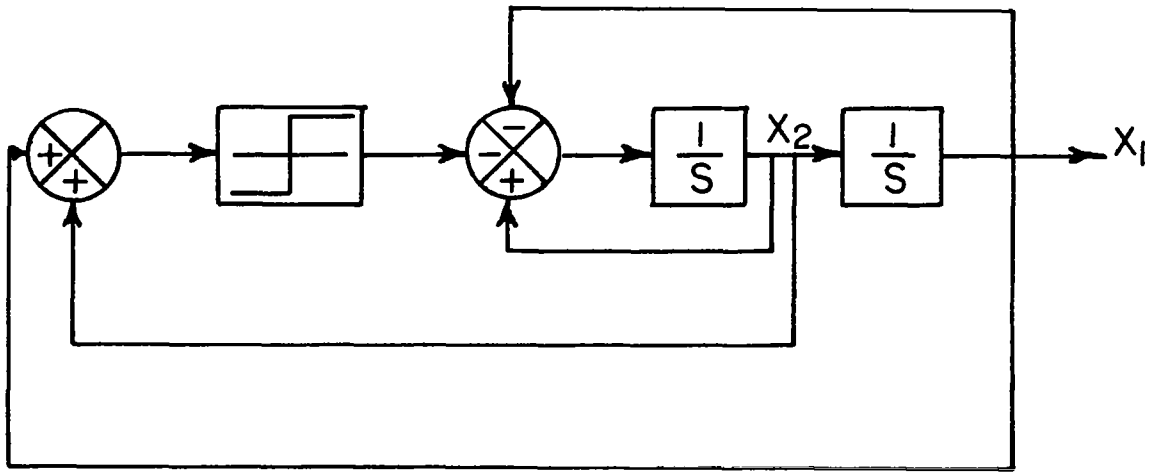

Fig. 4-3 The System of Example 4-2.

initially as the identity matrix. Figure 4-4 gives the results of the search process together with the true (closed) boundary, approximated well by the computed boundary. The true boundary may be found by changing the sign of time in the differential equations and integrating them forward with a machine integration routine to obtain the stable limit cycle which the stability boundary becomes under the transformation of time; this limit cycle may also be determined analytically. The computed optimum H was

$$H = \begin{bmatrix} 2.89 & -1.05 \\ -1.05 & 1.68 \end{bmatrix}$$

with $C_{max} = 1.759$.

In this problem a phenomenon appears which degrades the convergence of the search process near the optimum. Two kinds of tangencies occur in general for these systems: a normal or "smooth" tangency which was illustrated in Figure 3-1 and a "corner" tangency, a contact between $V = \text{const.}$ and $\dot{V} = 0$ surfaces on $\sigma = 0$, illustrated in Figure 3-3. (As mentioned in Chapter III, the $\dot{V} = 0$ surface is described more accurately as the boundary between regions of $\dot{V} < 0$ and $\dot{V} > 0$, since $\dot{V}$ changes sign discontinuously across this surface when it coincides with $\sigma = 0$). The smooth tangency is found by using the tangency search with (3-3) and (3-9a) with $\sigma \neq 0$. The corner tangency may be found similarly by replacing $\text{sgn}(\sigma)$ with $\tanh(\alpha\,\sigma)$ in (3-3) and (3-9a) (α is a large positive constant), thus approximating the corner tangency by a smooth one. More accurately, a separate tangency search may be performed on $\sigma = 0$; this amounts to finding tangency between

$$V = \frac{1}{2}\,\underline{x}^T H \underline{x} \tag{4-5}$$

and

$$\dot{V} = \frac{1}{2}\,\underline{x}^T Q \underline{x} \pm \underline{k}^T \underline{x} + \underline{d}^T \underline{b} = 0$$

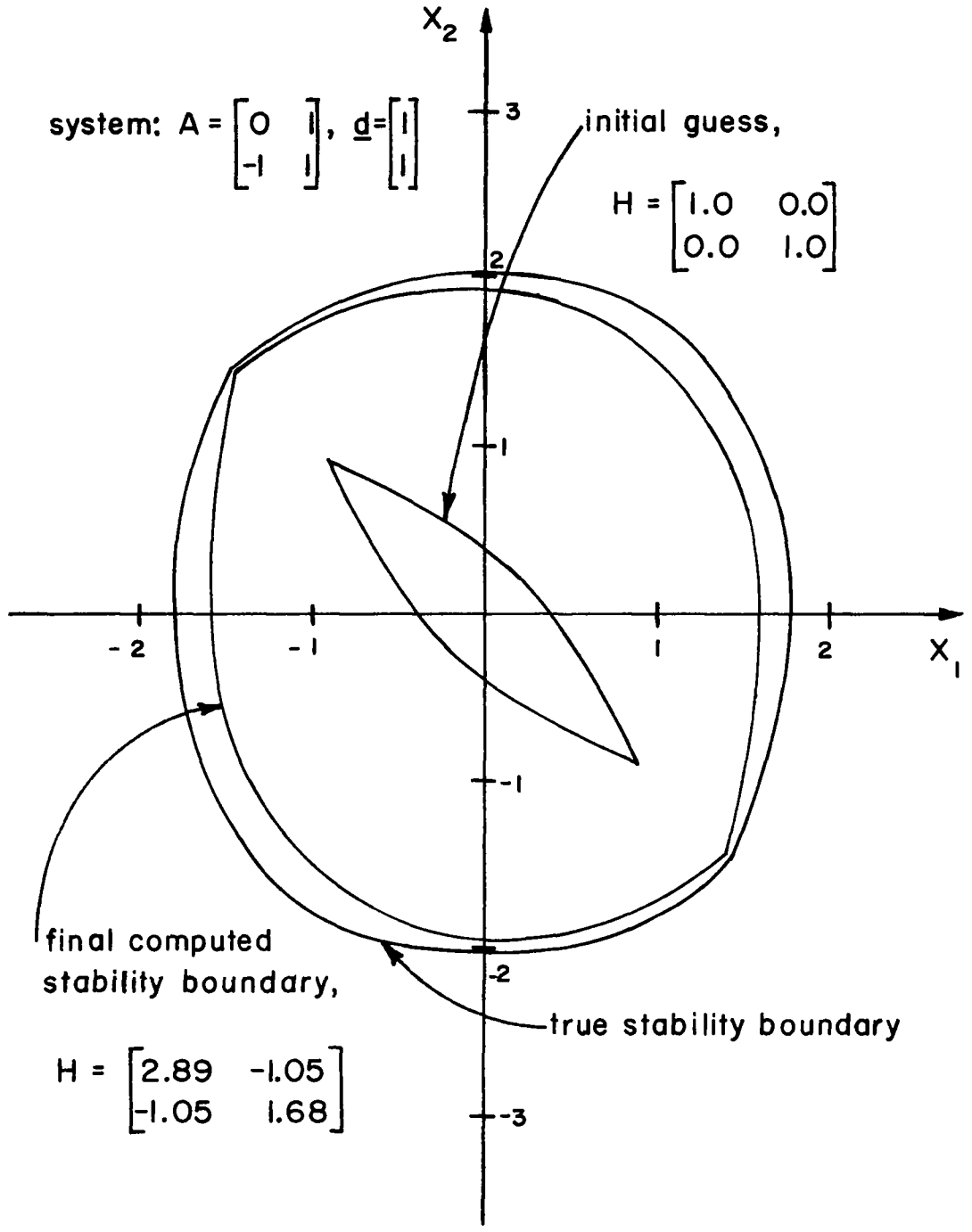

Fig. 4-4 Stability Boundaries for Example 4-2.

in the subspace

$$\underline{d}^T\underline{x} = 0$$

where the $\pm$ sign arises by examining $\dot{V}$ a small distance to either side of the switching surface. This latter procedure was the one used for these second-order examples, where it reduces simply to the solution of a quadratic, and thus does not require use of the tangency-search program.

A typical corner tangency for this example is illustrated in Figure 4-5. In Figure 4-6 the area I is plotted as a function of H_{11} for the H_{12} and H_{22} of Figure 4-5. All those points to the left of the peak correspond to corner tangencies; to the right of the peak the tangencies are smooth. The result of the two types of tangencies is thus a sharp ridge (shown only in one dimension in Figure 4-6) in the performance measure I . The search procedure drives towards the ridge, "chatters" slowly on it toward the optimum, and then terminates prematurely.

Performance can be improved in several ways. First the alternative use of $\tanh(\alpha\,\sigma)$ for $\mathrm{sgn}(\sigma)$ has the effect of rounding the ridges and speeding convergence. Second, the search technique could be made sophisticated enough to follow sharp ridges. The procedure used in this example in effect followed the second course: when a computation terminated after chattering in small steps along a ridge, the direction of the ridge was estimated from the average direction of the chattering motion and a new computation begun after taking a large step along the ridge. The path in the H_{11} , H_{22} plane for this example is shown in Figure 4-7.

Fortunately these ridges are usually not reached until the stability region is fairly well approximated. Ingwerson points out [12]that the proximity between the curves $V = C_{max}$ and $\dot{V} = 0$ is a rough measure of goodness of the approximation of the stability domain; a point on the ridge corresponds to $V = C_{max}$ and $\dot{V} = 0$ curves with four points of contact, rather than the usual two, thus probably producing a good estimate.

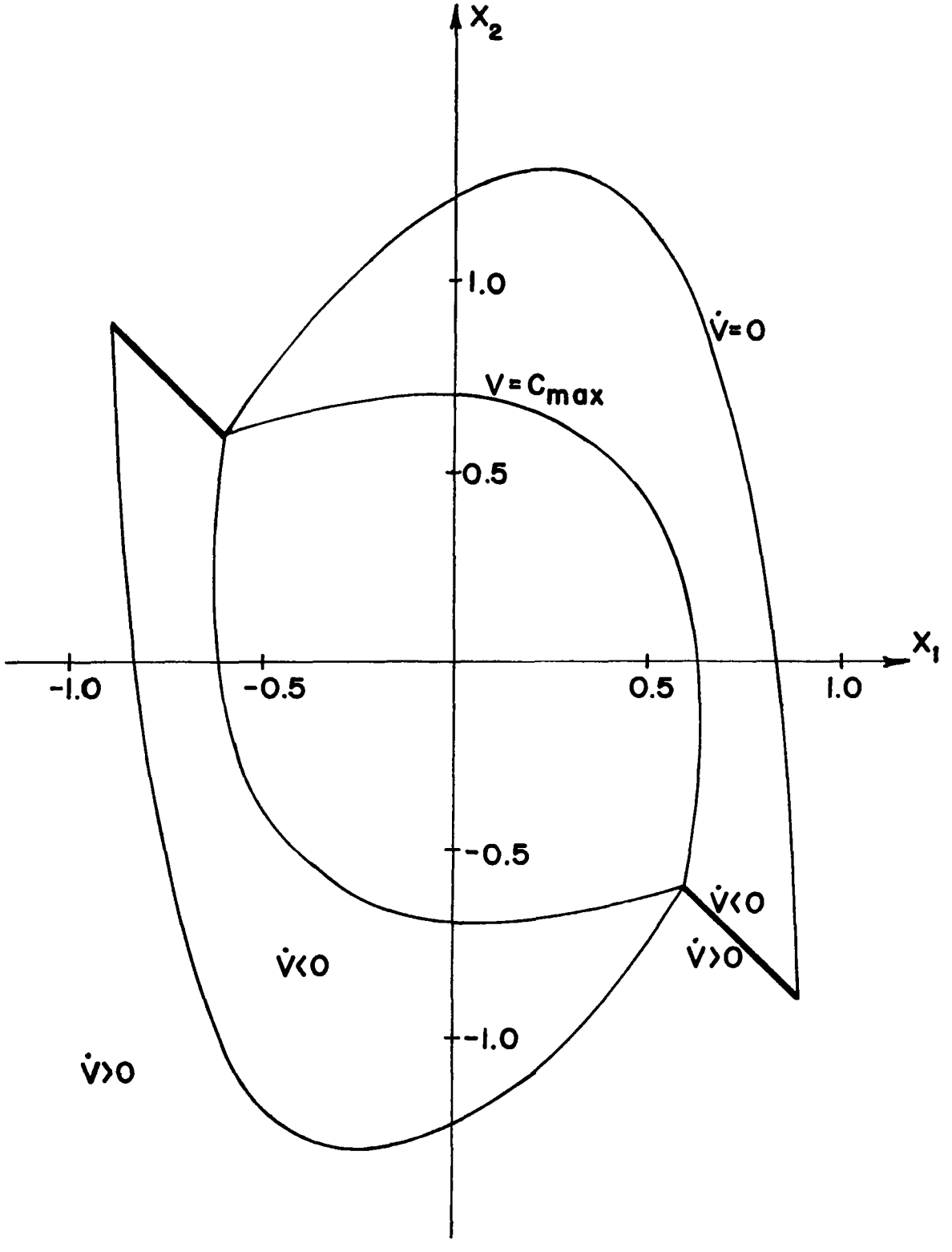

Fig. 4-5 Typical Corner Tangency for Example 4-2.

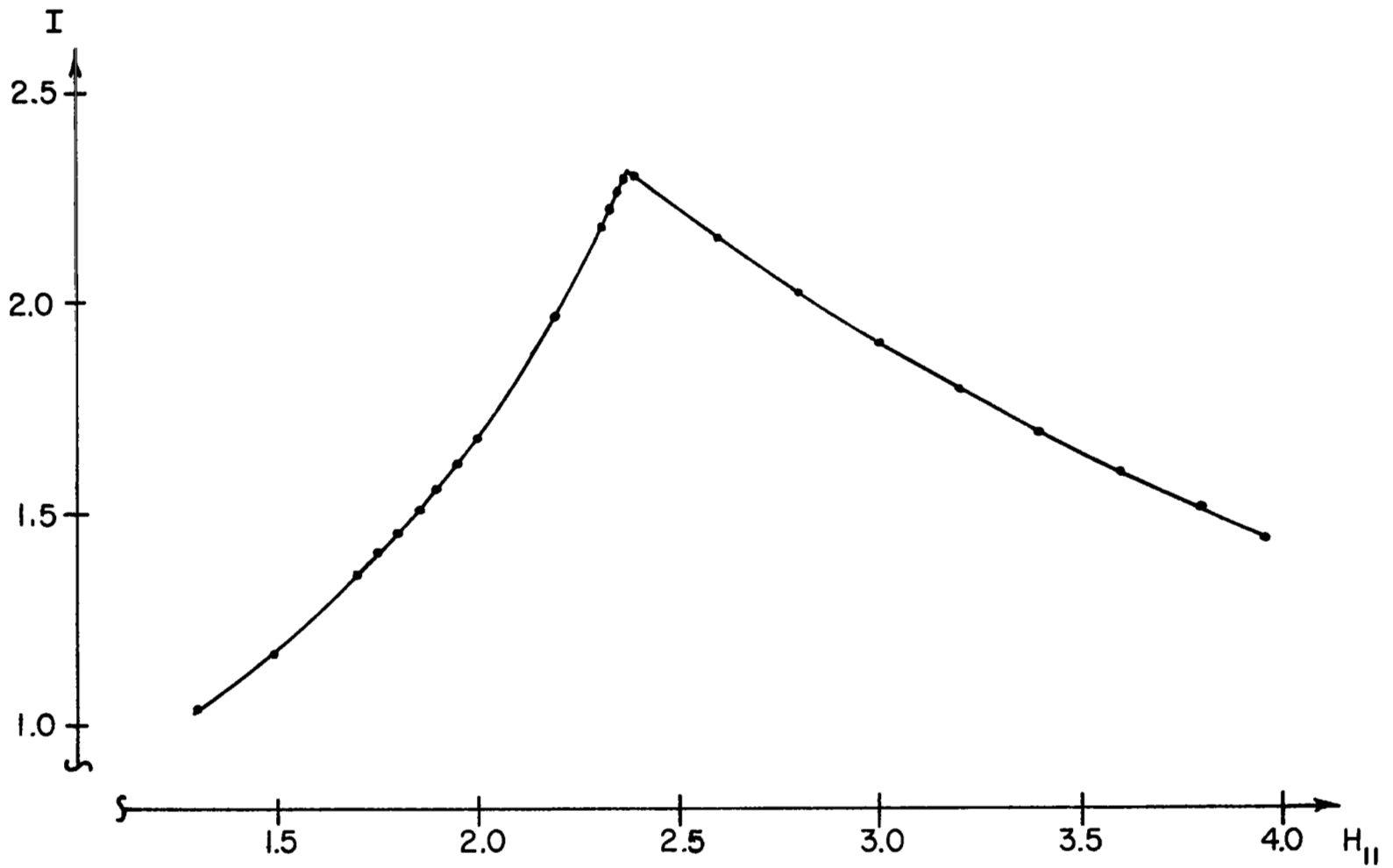

Fig. 4-6 Area Versus H_{11} for H_{12} and H_{22} of Figure 4-5.

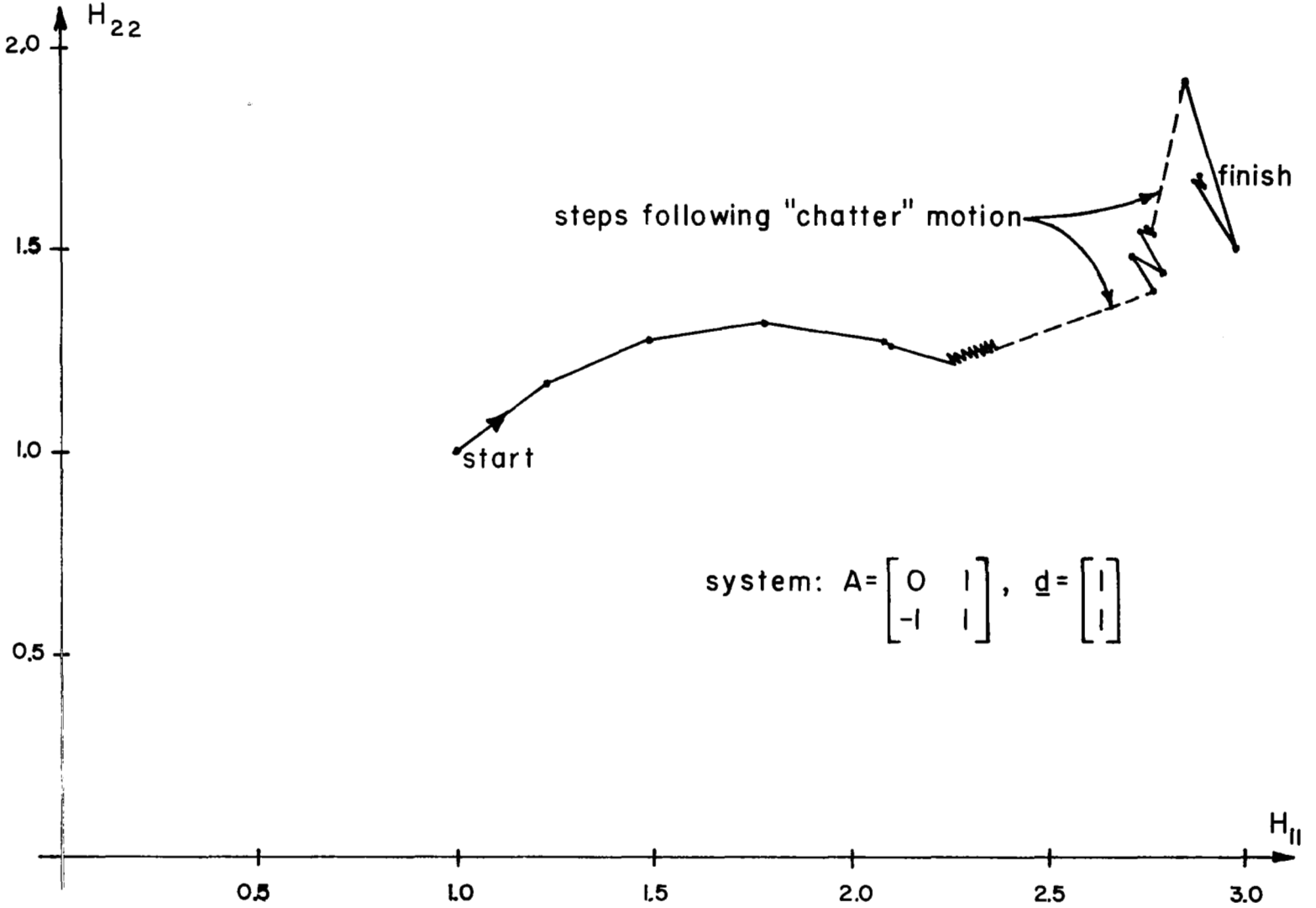

Fig. 4-7 Motion of the Parameter Point in the H_{11}-H_{22} Plane for Example 4-2.

Example 4-3

Consider the system

$$\dot{x}_1 = x_2$$

$$\dot{x}_2 = - x_1 - \text{sgn}(2x_1 + x_2) \tag{4-6}$$

By examining the terms of V and $\dot{V}$ in detail one finds rather easily that the Lyapunov function

$$V = \frac{1}{2} \underline{x}^T \begin{bmatrix} 3.0 & 0 \\ 0 & 3.0 \end{bmatrix} \underline{x} + (2x_1+x_2)\text{sgn}(2x_1+x_2) \tag{4-7}$$

demonstrates the system to be asymptotically stable in the large.

H was again taken initially as the identity matrix. The results are shown in Figure 4-8; the final H was

$$H = \begin{bmatrix} 1.57 & - 0.24 \\ - 0.24 & 1.53 \end{bmatrix}$$

with the boundary given by $C_{max} = 20.44$. Although this computed H was not close to the H of (4-7) (which is unique among functions of the form (3-3) in proving global asymptotic stability) the estimate obtained might be useful for some purposes. This estimate could also probably be improved by further refinements in the computation process.

Example 4-4

Let the system be given by*

$$\dot{x}_1 = x_2$$

$$\dot{x}_2 = x_1 - x_2 - \text{sgn}(x_1) \tag{4-8}$$

*The uncontrolled system is that of Example 4-1 with the addition of some damping; the roots are $- 1/2 \pm \sqrt{5}/2$.

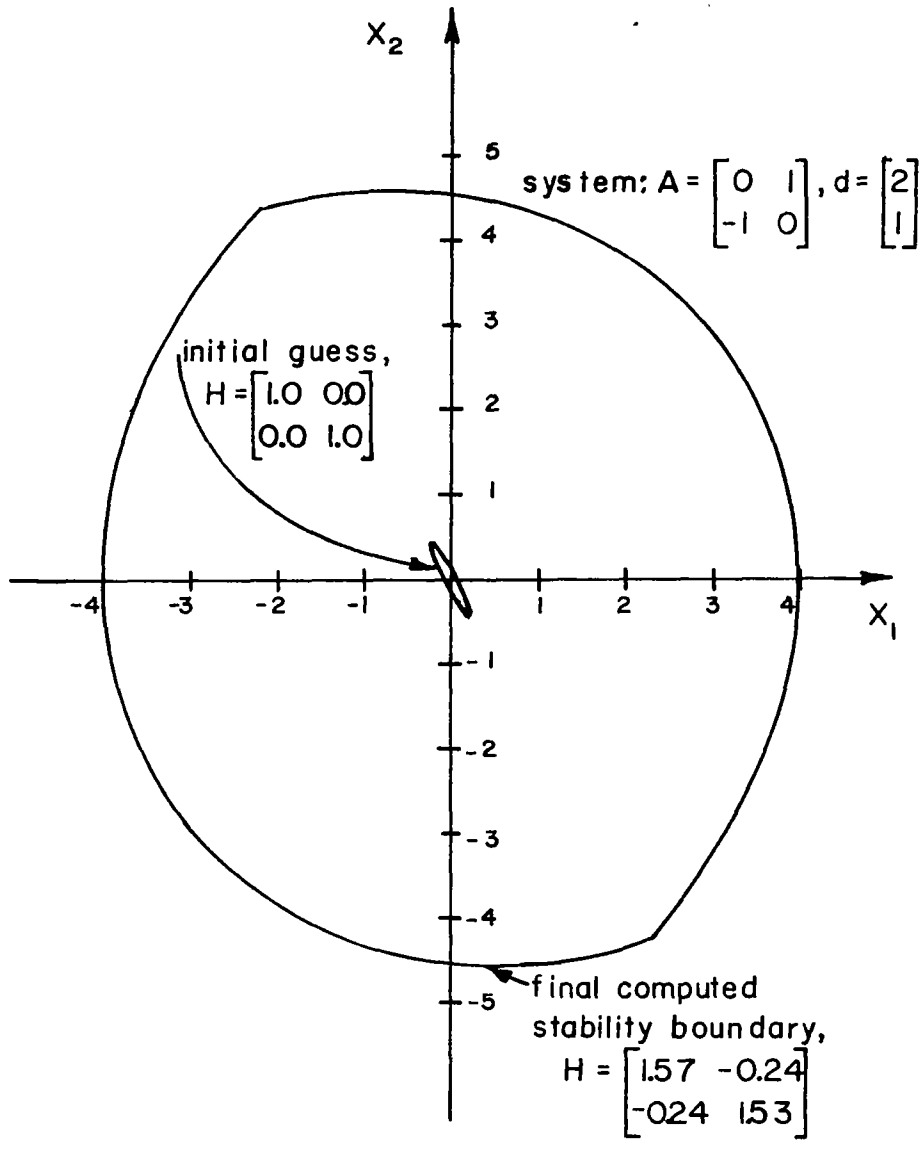

Fig. 4-8 Stability Boundaries for Example 4-3.

No sliding motions exist since $\underline{d}^T\underline{b} = 0$. An analysis of $\dot{V}$ readily shows that for (3-3) to be a Lyapunov function for (4-8) it is necessary that

$$H_{22} = 1 \tag{4-9}$$

and

$$1 > H_{12} > 0$$

H_{22} was therefore held fixed at unity and the search was begun at

$$H = \begin{bmatrix} 1.0 & 0.5 \\ 0.5 & 1.0 \end{bmatrix}$$

The search remained in the allowable region (4-9) without further constraints with the resulting H ,

$$H = \begin{bmatrix} 0.50 & 0.89 \\ 0.89 & 1.00 \end{bmatrix}$$

producing the boundary shown in Figure 4-9 with $C_{max} = 1.229$.

Example 4-5

Consider the plant of Example 4-1 with a new switching function

$$\dot{x}_1 = x_2$$

$$\dot{x}_2 = x_1 - sgn(x_1 + x_2) \tag{4-10}$$

An examination of phase-plane trajectories readily shows that this system is A. S. in the infinite strip bounded by $x_1 + x_2 = \pm 1$. With this result in mind it is easy to show (by a detailed study of the terms of V and $\dot{V}$) that the Lyapunov function

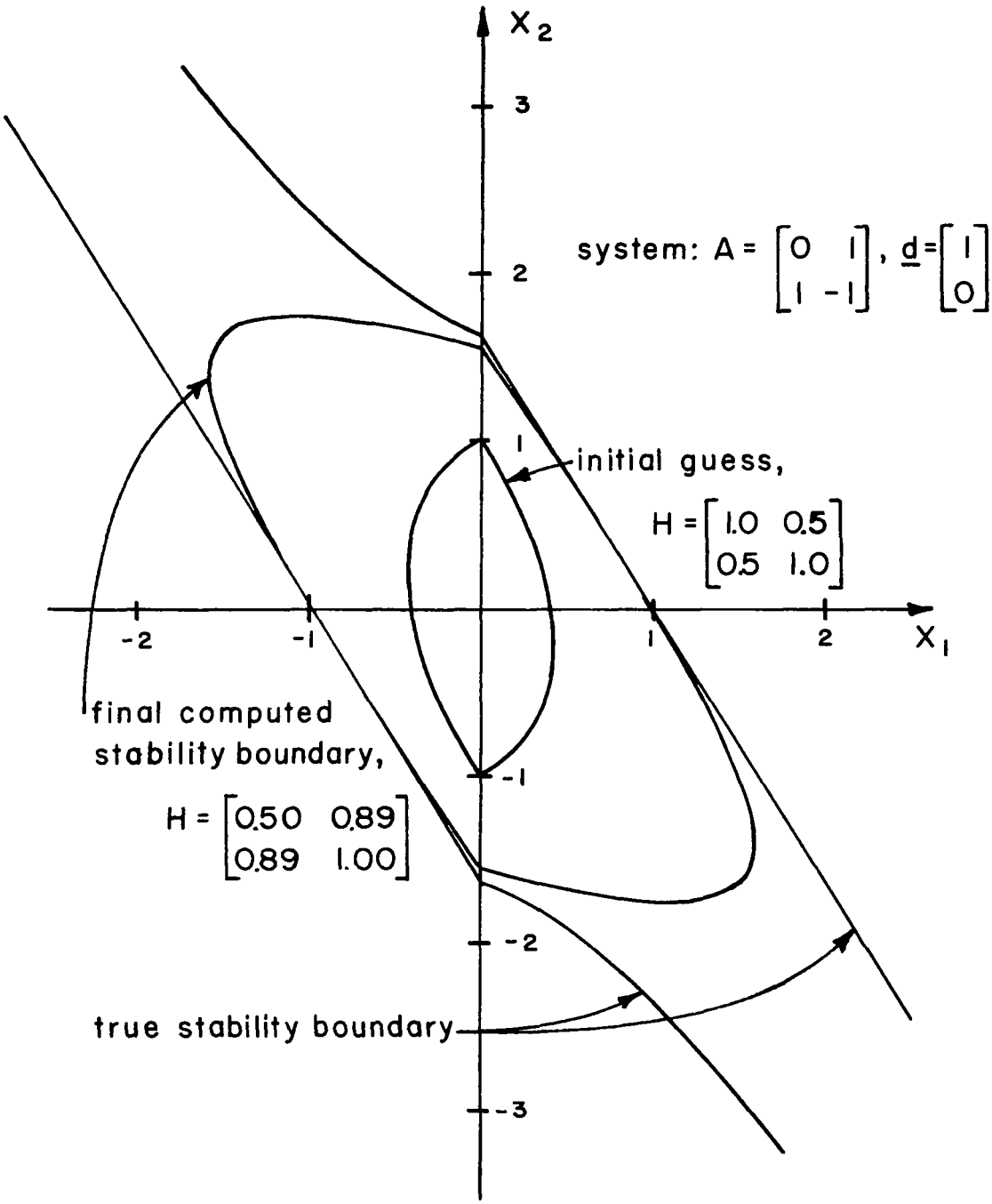

Fig. 4-9 Stability Boundaries for Example 4-4.

$$V = \frac{1}{2}\underline{x}^T \begin{bmatrix} (1+\epsilon) & 1 \\ 1 & 1 \end{bmatrix} \underline{x} + (x_1 + x_2)\mathrm{sgn}(x_1 + x_2) \qquad (4\text{-}11)$$

provides an arbitrarily large estimate of the stability region for sufficiently small positive ϵ . In the limiting case of $\epsilon = 0$, $V = C_{max}$ and $\dot{V} = 0$ coincide but V becomes semi-definite and thus not a proper Lyapunov function.

The results of the search process, starting again with $H = I$, are shown in Figure 4-10. The computed H was

$$H = \begin{bmatrix} 0.70 & 0.73 \\ 0.73 & 0.82 \end{bmatrix}$$

with $C_{max} = 1.234$.

Example 4-6

Consider now a system with a non-linear plant, shown in Figure 4-11,

$$\dot{x}_1 = x_2$$

$$\dot{x}_2 = x_1^3 - \mathrm{sgn}(2x_1 + x_2) \qquad (4\text{-}12)$$

The computed H was

$$H = \begin{bmatrix} 0.88 & 0.11 \\ 0.11 & 1.30 \end{bmatrix}$$

with the results shown in Figure 4-12. The boundary was given by $C_{max} = 2.111$. The true boundary was found by integrating (4-12) backward from final conditions determined from an examination of graphically constructed trajectories. The quality of the estimate and the speed of convergence of the search were not as good as for the related linear plant of Example 4-1.

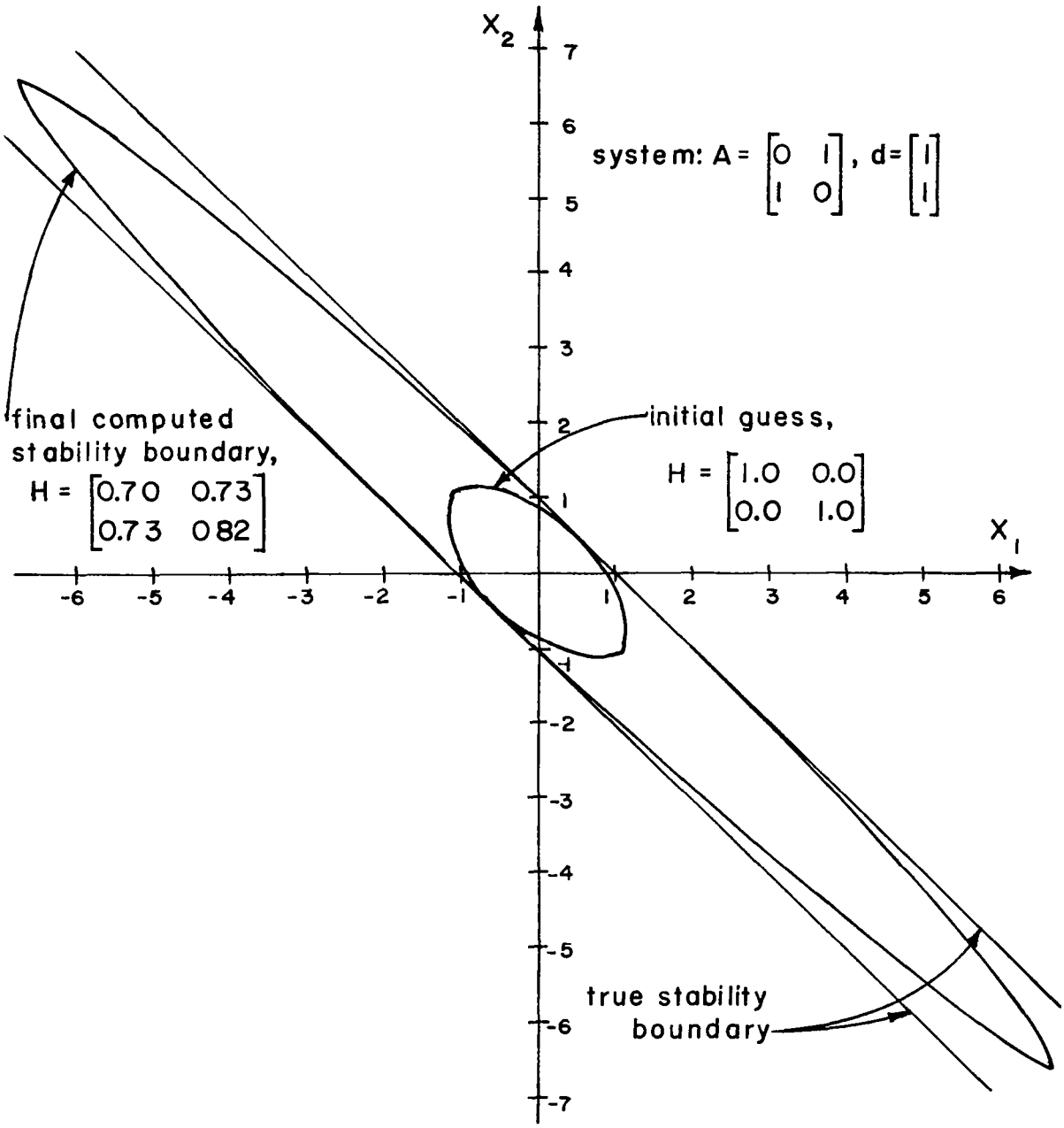

Fig. 4-10 Stability Boundaries for Example 4-5.

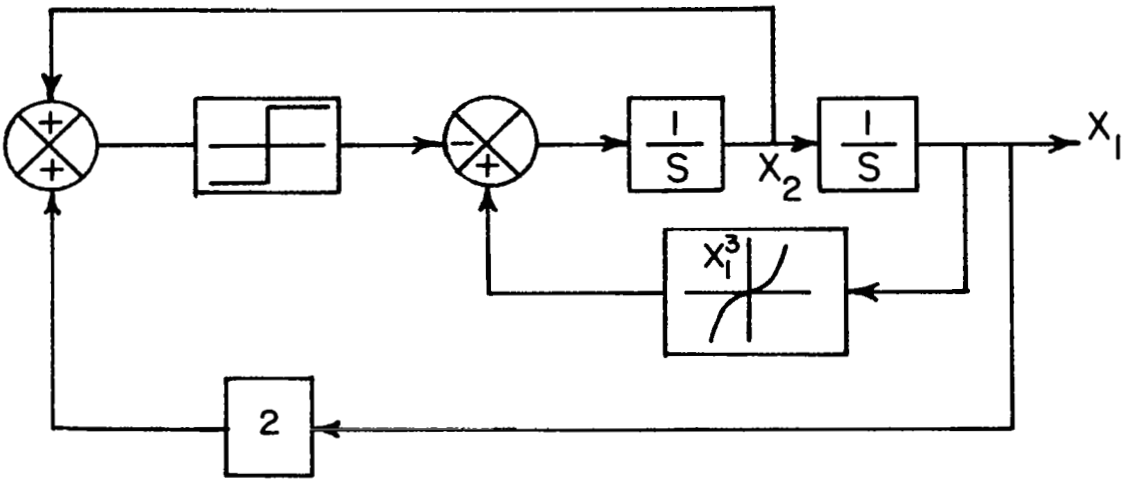

Fig. 4-11 The System with Non-linear Plant of Example 4-6.

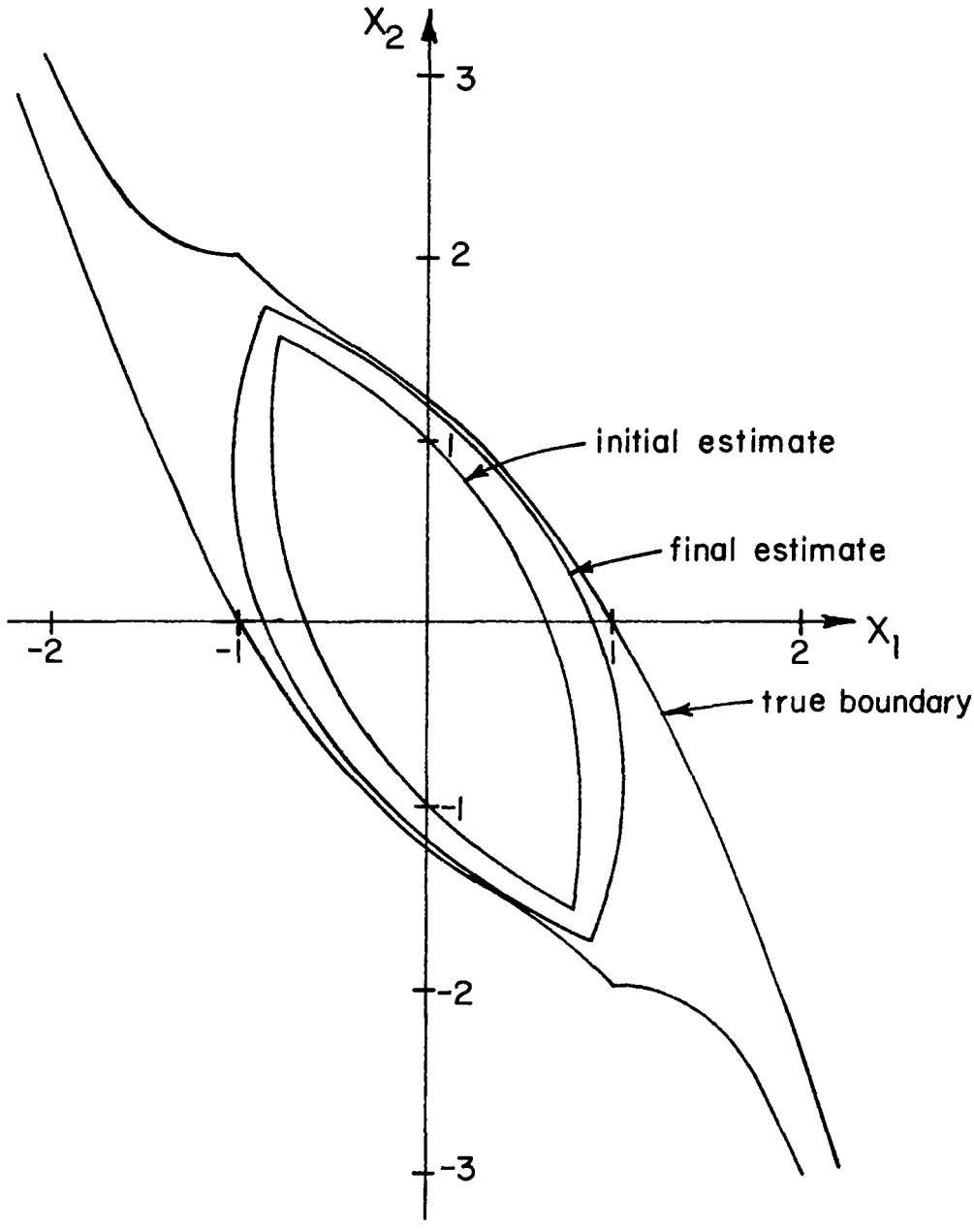

Fig. 4-12 Stability Boundaries for Example 4-6.

4. THIRD-ORDER EXAMPLES

Example 4-7

Consider the system

$$\dot{x}_1 = x_2$$

$$\dot{x}_2 = x_3 \qquad (4\text{-}13)$$

$$\dot{x}_3 = -.5x_1 - .5x_2 + .5x_3 - \text{sgn}(x_1 + 2x_2 + x_3)$$

shown in block-diagram form in Figure 4-13. For third-order problems the corner tangency was determined by finding a two-dimensional smooth tangency for Equations (4-5) using the tangency-search program. Again H was initially chosen as the identity matrix. The results for this problem are illustrated in Figure 4-14, with the initial estimate pictured above the computed estimate. The regions are indicated by plotting the intersection curve of the surface $V = C_{max} = 1.136$ on the switching plane; superimposed on this are curves of the intersection of $V = C_{max}$ and planes $x_3 = \text{constant}$. The x_1 and x_2 axes are oriented and scaled to give the x_1,x_2 coordinates of points on the curves $x_3 = \text{constant}$. The x_3 axis is scaled differently to give the x_3 coordinates of points on the switching plane. This view is not a perspective one; it has been constructed to show the true area of the cross-sections indicated. As a guide, the coordinates of a sample point P on $V = C_{max}$ are shown in Figure 4-14. The x_1,x_2 coordinates are obtained directly from the x_1,x_2 projections, while the x_3 coordinate (which is the same for all the points P , P_1 , P_{s1} and P_{s2}) is obtained from the intersection of the x_3 axis and the line connecting the points P_{s1} and P_{s2} , those points on the closed curve which lie on the switching plane.

The computed H was

$$H = \begin{bmatrix} 0.78 & 0.73 & -0.88 \\ 0.73 & 1.04 & -0.66 \\ -0.88 & -0.66 & 1.77 \end{bmatrix}$$

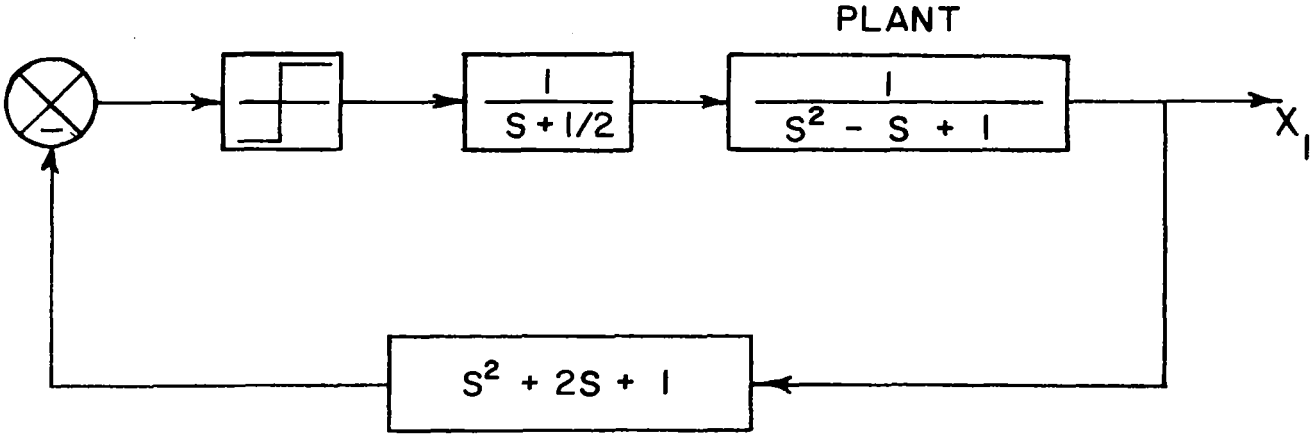

Fig. 4-13 Third-Order System of Example 4-7.

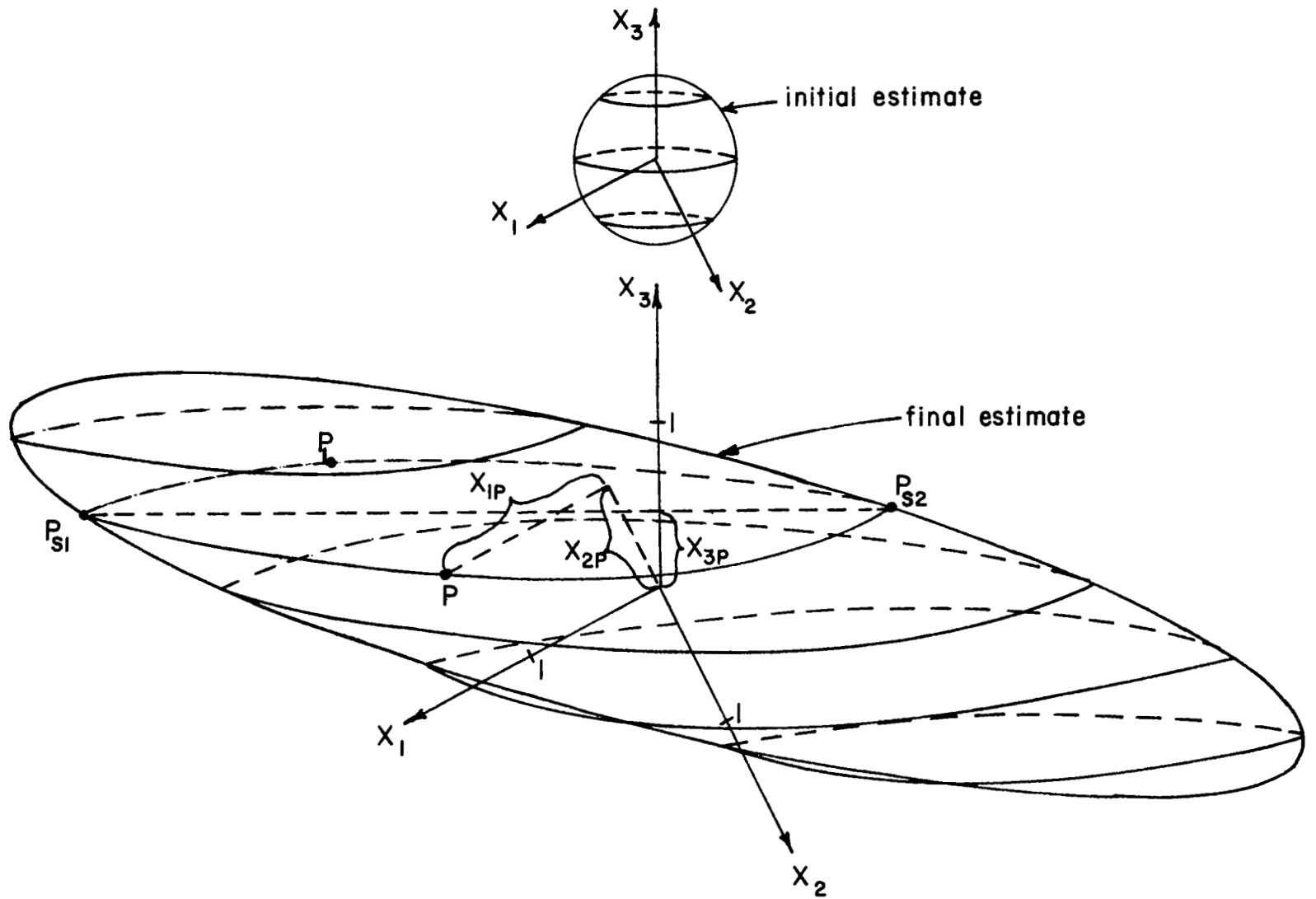

Fig. 4-14 Initial and Computed Stability Boundaries of Example 4-7.

The negative definiteness of $\dot{V}_s$ was verified at the end of the computation by evaluating the eigenvalues of Q' (see Equation (3-33)), which were $-.082$ and -7.73 .

Example 4-8

Consider the system of the last example, but now with the damping ratio of the plant (see Figure 4-13) decreased from $-1/2$ to -1 :

$$\begin{aligned} \dot{x}_1 &= x_2 \\ \dot{x}_2 &= x_3 \\ \dot{x}_3 &= -.5x_1 + 1.5x_3 - \operatorname{sgn}(x_1 + 2x_2 + x_3) \end{aligned} \tag{4-14}$$

The results of the search, starting again with $H = I$, are shown in Figure 4-15. The boundary was given by $C_{max} = 0.232$ with

$$H = \begin{bmatrix} 0.79 & 0.66 & -0.82 \\ 0.66 & 0.94 & -0.39 \\ -0.82 & -0.39 & 1.72 \end{bmatrix}$$

The eigenvalues of Q' were -0.775 and -3.225 .

Example 4-9

Consider the velocity-controlled, second-order plant of Example 4-1 shown in the block diagram of Figure 4-16. The differential equation is

$$\begin{aligned} \dot{x}_1 &= x_2 \\ \dot{x}_2 &= x_3 \\ \dot{x}_3 &= x_2 - \operatorname{sgn}(.33x_1 + 1.33x_2 + x_3) \end{aligned} \tag{4-15}$$

The initial and final estimates are shown in Figures 4-17 and 4-18 with final $C_{max} = 1.295$ and

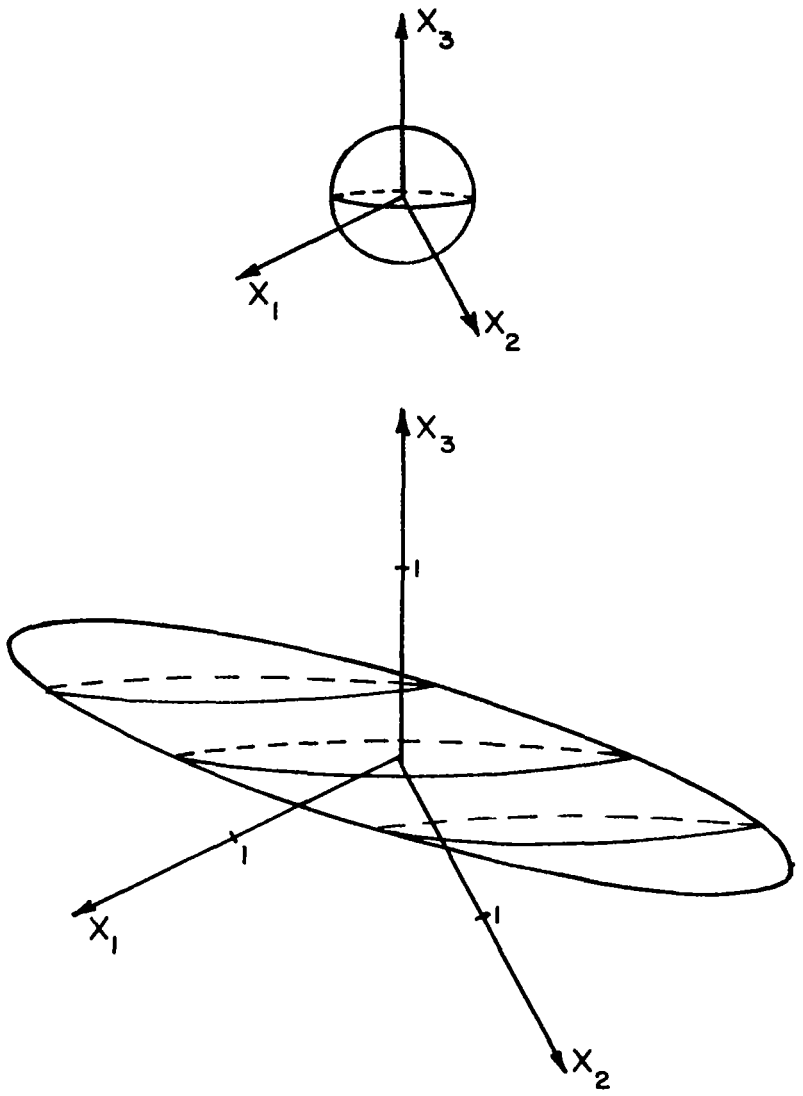

Fig. 4-15 Initial and Computed Stability Boundaries of Example 4-8.

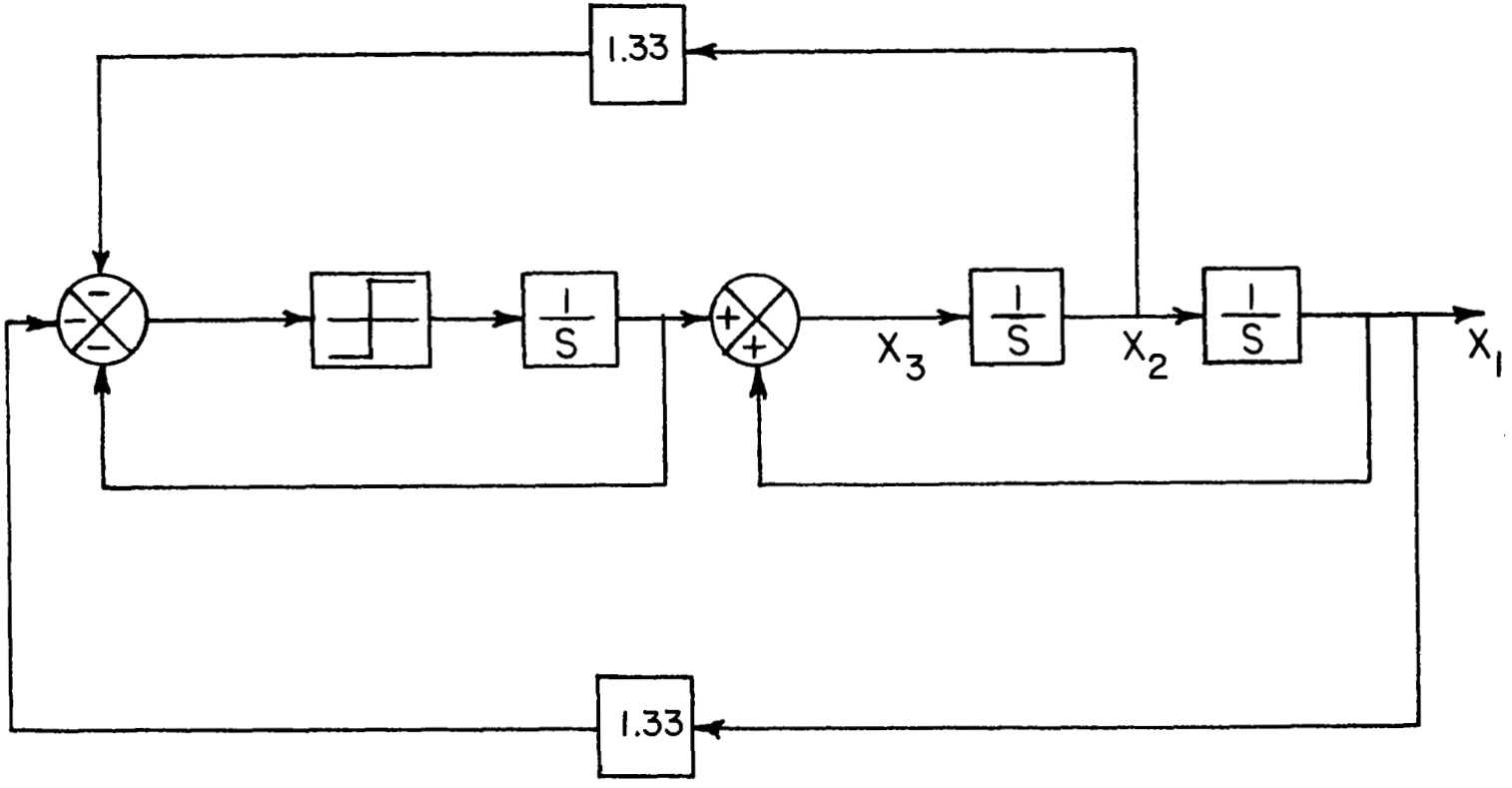

Fig. 4-16 Third-Order System of Example 4-9.

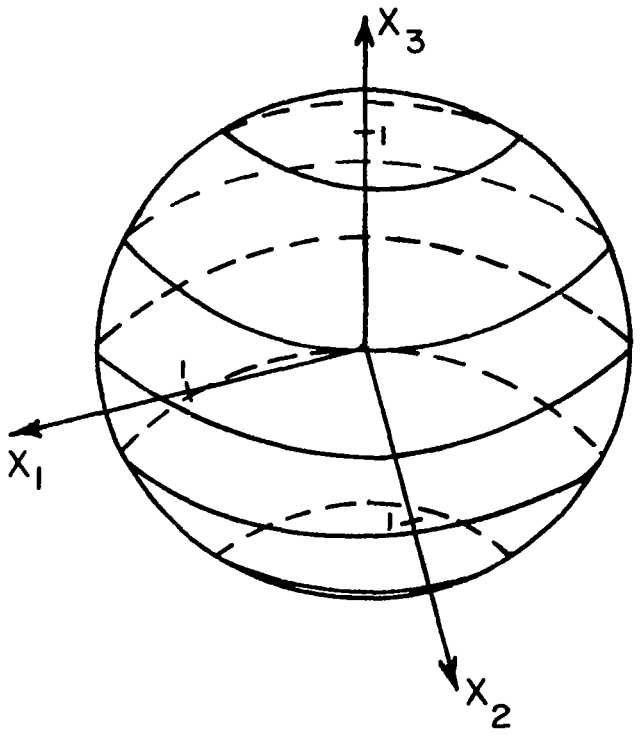

Fig. 4-17 Initial Boundary of Example 4-9.

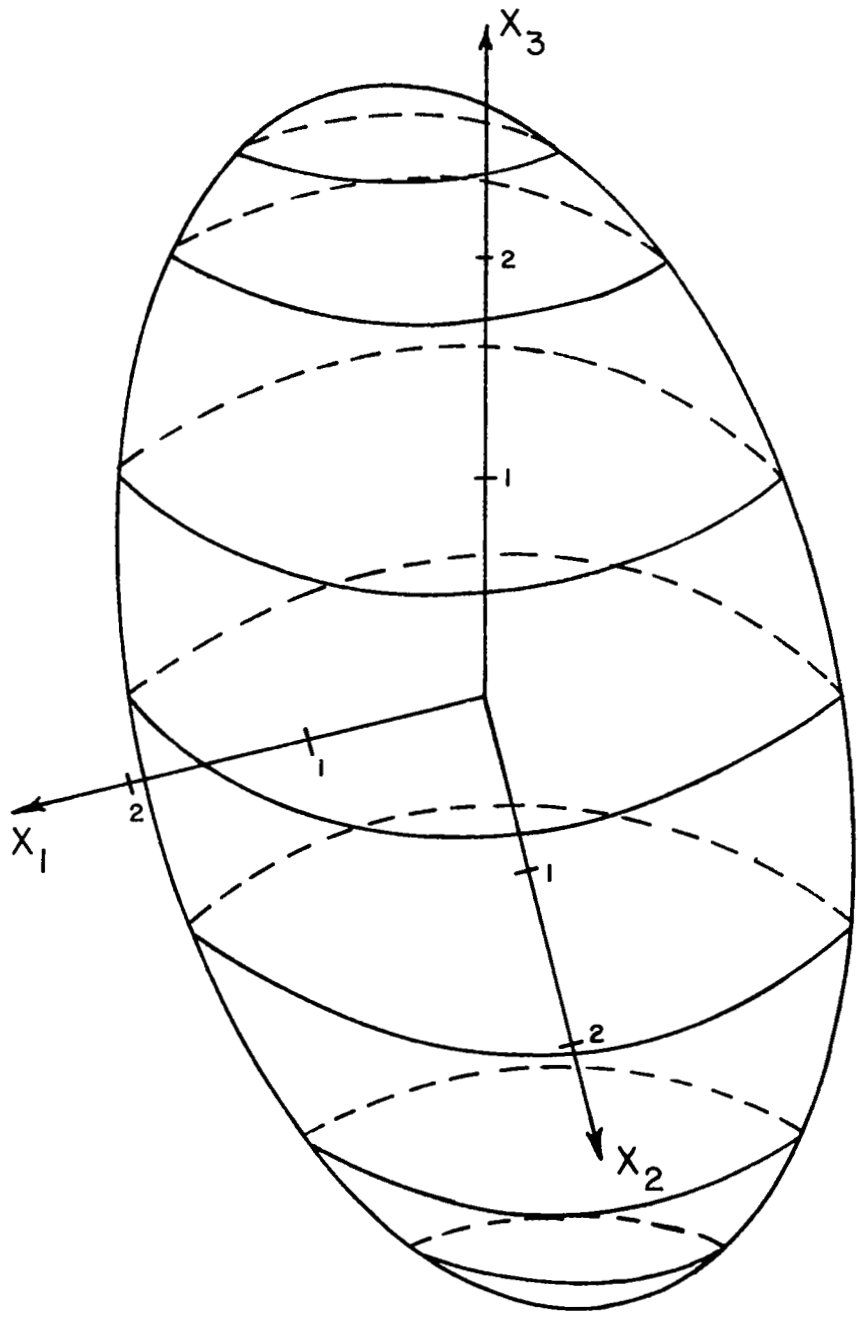

Fig. 4-18 Final Boundary of Example 4-9.

$$H = \begin{bmatrix} 0.62 & -0.11 & -0.06 \\ -0.11 & 0.75 & 0.68 \\ -0.06 & 0.68 & 0.93 \end{bmatrix}$$

The eigenvalues of the final Q' were $-.25$ and -2.41 .

Example 4-10

Consider again the plant of the last example, this time controlled with the switching function

$$\underline{d}^T\underline{x} = x_1 + 2x_2 + x_3 \qquad (4\text{-}16)$$

The initial and final estimates are shown in Figure 4-19. The boundary was given by $C_{max} = 1.023$ with

$$H = \begin{bmatrix} 1.16 & 0.29 & -0.96 \\ 0.29 & 0.80 & 0.35 \\ -0.96 & 0.35 & 1.26 \end{bmatrix}$$

The eigenvalues of Q' were -0.026 and -4.373 .

It should be pointed out that the best possible stability-domain estimate is actually the union of all of the estimates obtained in the course of a computation. Although this union was sometimes greater than the final estimate by itself, it was not sufficiently different to justify its calculation.

5. NON-LINEAR SWITCHING

This method may be extended to systems with non-linear switching functions in several ways. First it is possible in many cases to find a non-linear transformation from $\underline{x}$ to $\underline{u}$ coordinates such that $\sigma(\underline{x}) = \underline{d}^T\underline{u}$ and (2-1) becomes

$$\dot{\underline{u}} = \underline{F}'(\underline{u}) + \underline{c}'(\underline{u})\mathrm{sgn}(\underline{d}^T\underline{u}) \qquad (4\text{-}17)$$

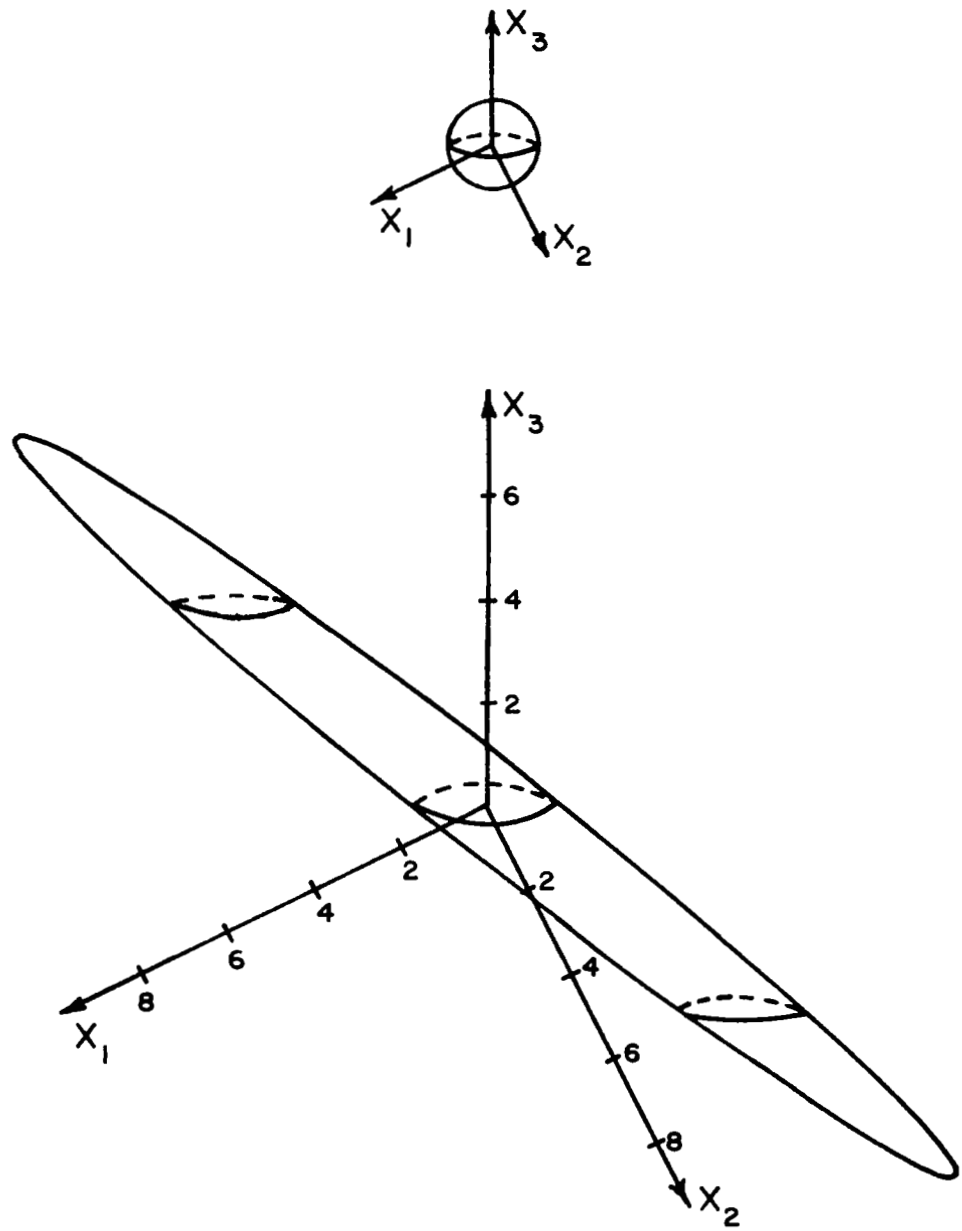

Fig. 4-19 Initial and Final Boundaries of Example 4-10.

so that the construction may proceed as in Example 4-6. Second, the V function

$$V = \frac{1}{2} \underline{x}^T H \underline{x} + \sigma \text{ sgn } \sigma \tag{4-18}$$

could be used directly. As mentioned earlier, however, an exact integration for the volume within $V = C_{max}$ for (4-18) is in general impossible and a close numerical approximation to the volume can be obtained only at the expense of large amounts of computer time for third- and higher-order systems. A more reasonable approach, and one with wider application, is to replace the exact volume with a simpler figure of merit, a "quasi-volume." An example is the sum of the square magnitudes of $\underline{x}$ on $V = C_{max}$ in selected directions in state space. Such a measure would still be positive definite and give a rough measure of the volume, without requiring extensive calculations. It would also have the advantage of being readily implemented for high-order systems where a computation of the exact volume, even for linear switching, is not simple.

V. EXTENSIONS OF THE STEEPEST-ASCENT METHOD

1. SYSTEMS WITH SATURATION

In general, physical controllers all possess the characteristic of saturation: there is a maximum level of control effort which cannot be exceeded. The relay controllers which have been discussed so far are limiting cases of such controllers, where the non-saturating region of operation vanishes. In many practical controllers, however, the device operates over a significant range at less than its maximum effort; the most simple and frequently used idealization of such devices is the saturation function of Equation (2-6) shown in Figure 5-1.

If we replace the signum function in the system of Equation (2-3) with the saturation function the new system can be expressed as

$$\dot{\underline{x}} = A\underline{x} + \begin{cases} k\underline{b}\underline{d}^T\underline{x} , & |\underline{d}^T\underline{x}| \leq \frac{1}{k} \\ \underline{b}\ \text{sgn}\ \underline{d}^T\underline{x} , & |\underline{d}^T\underline{x}| > \frac{1}{k} \end{cases} \tag{5-1}$$

or

$$\dot{\underline{x}} = \begin{cases} \tilde{A}\underline{x} , & |\underline{d}^T\underline{x}| \leq \frac{1}{k} \\ A\underline{x} + \underline{b}\ \text{sgn}\ \underline{d}^T\underline{x} , & |\underline{d}^T\underline{x}| > \frac{1}{k} \end{cases} \tag{5-2}$$

where $\tilde{A} = A + k\underline{b}\underline{d}^T$.

In analogy to our treatment of (2-3) we again consider the use of the Lur'e form of V function for the new system (5-2). Keeping in mind the definition of V as a quadratic plus the integral of the non-linearity we can write

$$V = \frac{1}{2}\underline{x}^T H\underline{x} + \begin{cases} \frac{1}{2}k\sigma^2 , & |\sigma| \leq \frac{1}{k} \\ \sigma\ \text{sgn}\ \sigma - \frac{1}{2k} , & |\sigma| > \frac{1}{k} \end{cases} \tag{5-3}$$

where $\sigma = \underline{d}^T\underline{x}$.

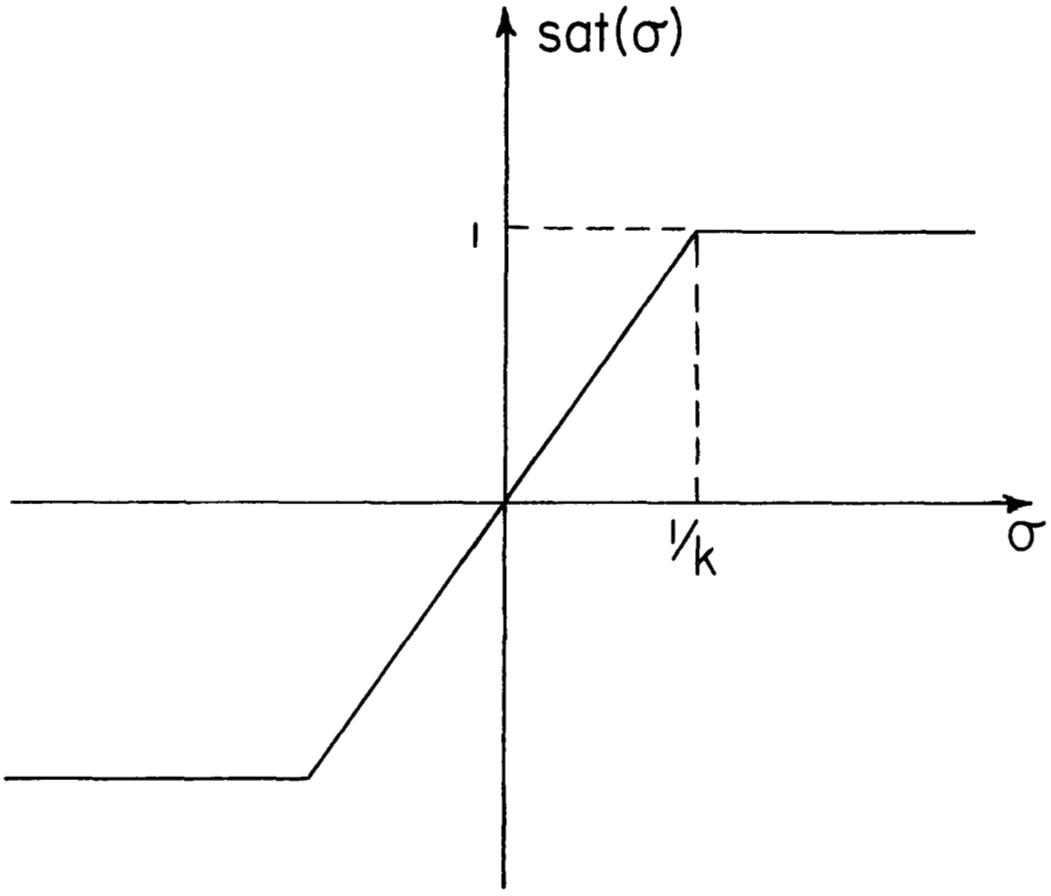

Fig. 5-1 The Saturation Function.

Equation (5-3) may be rewritten as

$$V = \begin{cases} \frac{1}{2}\underline{x}^T\tilde{H}\underline{x} & , \quad |\sigma| \le \frac{1}{k} \\ \\ \frac{1}{2}\underline{x}^T H\underline{x} + \sigma \operatorname{sgn}\sigma - \frac{1}{2k} & , \quad |\sigma| > \frac{1}{k} \end{cases} \tag{5-4}$$

where $\tilde{H} = H + k\underline{d}\underline{d}^T$.

Using (5-2), $\dot{V}$ can be evaluated to be

$$\dot{V} = \begin{cases} \frac{1}{2}\underline{x}^T\tilde{Q}\underline{x} & , \quad |\sigma| \le \frac{1}{k} \\ \\ \dot{V}_{(3\text{-}9a)} & , \quad |\sigma| > \frac{1}{k} \end{cases} \tag{5-5}$$

where $\tilde{Q} = \tilde{A}^T\tilde{H} + \tilde{H}\tilde{A}$ and $\dot{V}_{(3\text{-}9a)}$ denotes $\dot{V}$ according to (3-9a). Note that in the saturation region the only change in V and $\dot{V}$ from the relay-control analysis of Chapter III is a numerical decrease of the value of V by an amount $1/2k$; $\dot{V}$ is unchanged. Thus if we begin with a Lyapunov function and stability boundary computed for the relay-control system (2-3) we need only check the positive and negative definiteness of the $\tilde{H}$ and $\tilde{Q}$ matrices in order to obtain a stability boundary for the corresponding control system with a saturation characteristic now in place of the relay. The new boundary will match the relay boundary in the saturation region but will be modified in the linear region $|\sigma| < (1/k)$ with a rounding of the sharp corners.

It might at first be expected that if a function V (3-3) is a Lyapunov function for a relay-control system (2-3) then the function V (5-4) with the same H will also be a Lyapunov function for the saturation system (5-2) for sufficiently large k . It is easy to verify, however, that this is not true; the explanation is that $\tilde{H}$ becomes dominated by the terms containing k as it becomes large and thus V in the linear region comes to depend on the quadratic form $(1/2)\underline{x}^T k\underline{d}\underline{d}^T\underline{x}$, which is not necessarily a desirable choice. For example, the computed H's of Examples 4-1 and 4-2 do not produce Lyapunov functions of the form (5-4) for the corresponding systems with

saturation for k's of 2 and 5, particular values which were tested. However, the computed H of Example 4-4 does produce a Lyapunov function for the corresponding system with a saturation characteristic of $k = 2$. For this case,

$$\tilde{H} = \begin{bmatrix} 2.50 & 0.89 \\ 0.89 & 1.00 \end{bmatrix}$$

and

$$\tilde{Q} = \begin{bmatrix} -1.78 & -0.61 \\ -0.61 & -0.22 \end{bmatrix}$$

which may readily be demonstrated to be positive and negative definite, respectively. In order to compute the modified portion of the stability boundary, note from the second line of (5-4) that the new value of C_{max}, $\tilde{C}_{max}$, is

$$\tilde{C}_{max} = C_{max_0} - \frac{1}{2k} \qquad (5\text{-}6)$$

where C_{max_0} is the value for the relay-control system. For $k = 2$ and $C_{max_0} = 1.23$, $\tilde{C}_{max} = .98$ and the equation for the new portion of the boundary becomes

$$\frac{1}{2} \underline{x}^T \tilde{H} \underline{x} = .98 \quad , \qquad |x_1| < .5$$

The entire boundary is shown in Figure 5-2, together with the true one, found by graphically constructing the trajectory constituting the boundary. A comparison with Figure 4-9 shows that the small change in the stability-domain estimate of this system produced by the addition of the linear region in the controller characteristic reflects very well the small change in the actual domain.

Although the approach illustrated in this example worked well in this particular instance, as mentioned earlier it cannot be expected to

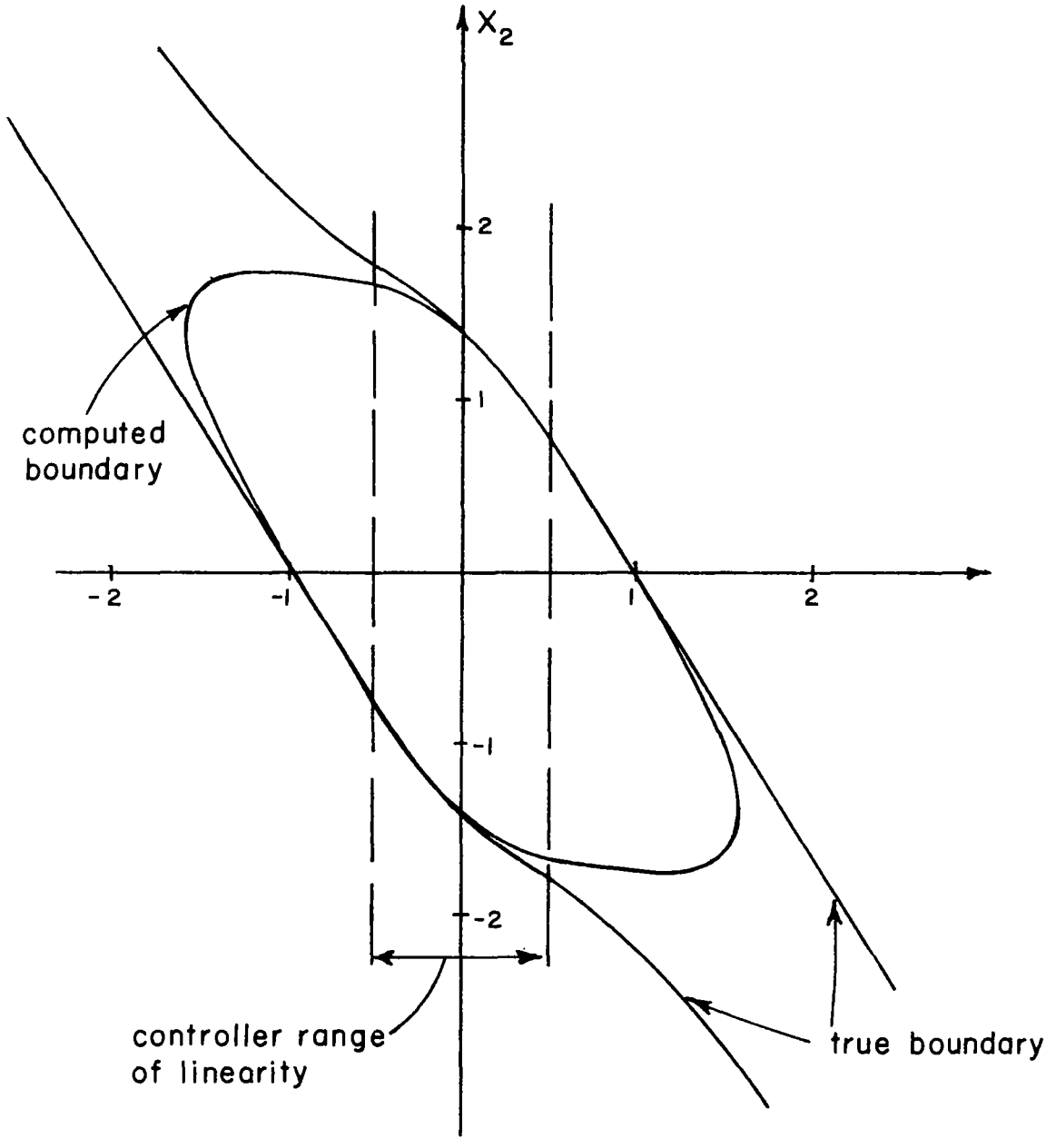

Fig. 5-2 Stability Boundaries for Example 5-1.

succeed in all cases. A better general policy is to optimize the volume directly for the function (5-4), choosing the starting H to make $\tilde{H}$ and $\tilde{Q}$ both definite initially. The area and volume computations of Appendix A and B can be easily modified to give the correct measurements of the volume I for second- and third-order systems.

2. GENERAL NON-LINEARITIES

This method of finding a "best" stability-boundary estimate by optimizing a fixed form of Lyapunov function may clearly be applied to systems with more general non-linearities than those considered until now. The only requirements are a Lyapunov function depending on a set of parameters (the Lur'e form may be taken as a simple, readily constructed example) and a method of measuring the volume. As mentioned in the last chapter, for complex non-linearities, a very coarse numerical approximation to the volume might serve adequately. (This problem would properly be the subject of further research.) It should be kept in mind, however, that increasing the complexity of the non-linearities will probably increase both the time spent in determining tangencies and in computing even simplified volumes.

A potentially useful application for smooth non-linearities would be the computation of the optimum simple quadratic boundary. (For non-linearities which have a Taylor series expansion the quadratic Lyapunov function holds a similar position as our function (3-3) does for the discontinuous system, e.g. for A. S. systems, a set of quadratic Lyapunov functions always exist to estimate the domain of asymptotic stability. [1]) It would be of interest to compare these results with ones obtained by Zubov's method for various numbers of iterations and initial choices of $\theta(\underline{x})$. Also, the optimum quadratic function found from the search process should be tried as the initial choice for the Zubov iteration in order to improve the convergence, which is very sensitive to this initial choice.

VI. CONCLUSIONS

The direct method of Lyapunov has been used in this thesis as a basis for a new, systematic technique for computing good estimates of the domain of asymptotic stability. This technique has been applied successfully to relay-control systems, whose discontinuous nature has excluded them in the past from analysis by the method of Zubov, the only other entirely systematic technique for constructing Lyapunov function estimates of the stability boundary. The principal advantages of this new method, as demonstrated in the useful numerical solutions found in numerous second- and third-order examples, are

1.) The method is ideally suited to high-speed machine computation.

2.) It is not restricted to low-order systems.

3.) The allowable form of non-linearities is quite general; they may, for example, be discontinuous or piecewise continuous as long as the resulting dynamical system is well-behaved. The only requirements are a Lyapunov function V depending on a set of adjustable parameters and a scheme for measuring the volume within $V = \text{constant}$. It is usually very easy to find such a Lyapunov function, the Lur'e form being a simple example.

4.) Because the performance index is improved by a steepest-ascent procedure, convergence to the optimum estimate is monotonic. This behavior compares favorably with the erratic convergence properties of Zubov's method. (A comparison is not entirely fair, however, since the method of Zubov does ultimately converge to the exact solution in problems in which it is applicable.)

Areas in which further work would be of interest are applications to fourth- and higher-order systems and a wider variety of non-linearities, employing simplified volume measures, and extensions of the method to vector-valued controls. This technique should also be considered as a possible adjunct to Zubov's method in determining an optimum quadratic form $\theta(\underline{x})$ to initiate Zubov's iteration process.

REFERENCES

1. W. Hahn, Theory and Application of Lyapunov's Direct Method, Prentice Hall, Englewood Cliffs, N. J., 1963.

2. J. LaSalle and S. Lefschetz, Stability by Lyapunov's Direct Method, Academic Press, New York, 1961.

3. R. E. Kalman and J. E. Bertram, "Control System Analysis and Design via the 'Second Method' of Lyapunov — Part I, Continuous — Time Systems," Journal of Basic Engineering, Trans. ASME, Series D, 82, pp. 371-393, June 1960.

4. J. J. Rodden, "Numerical Applications of Lyapunov Stability Theory," Ph.D. Dissertation, Division of Engineering Mechanics, Stanford University, Stanford, California, 1964. (Abbreviated version in preprints JACC, Stanford University, 1964, pp. 261-268.)

5. S. G. Margolis and W. G. Vogt, "Control Engineering Applications of V. I. Zubov's Construction Procedure for Lyapunov Functions," IEEE Transactions on Automatic Control, Vol. AC-8, pp. 104-133, April 1963.

6. I. Flügge-Lotz, Discontinuous Automatic Control, Princeton Press, Princeton, N. J., 1953.

7. M. Maltz, "Analysis of Chatter in Contactor Control Systems, with Applications to Dual-Input Plants," Ph.D. Dissertation, Stanford University, Stanford, California, 1963.

8. Yu. I. Alimov, "On the Application of Lyapunov's Direct Method to Differential Equations with Ambiguous Right Sides," Automation and Remote Control, Vol. 22, 7, pp. 713-725, December 1961.

9. A. A. Andronow and C. E. Chaikin, Theory of Oscillations, Princeton University Press, Princeton, N. J., 1949.

10. D. V. Anosov, "Stability of the Equilibrium Positions of Relay Control Systems," Automation and Remote Control, Vol. 20, 2, pp. 130-143, February 1959.

11. D. R. Ingwerson, "A Modified Lyapunov Method for Non-Linear Stability Analysis," IRE Transactions on Automatic Control, Vol. AC-6, pp. 199-210, May 1961.

12. D. R. Ingwerson, "A Modified Lyapunov Method for Non-Linear Stability Problems," Ph.D. Dissertation, Division of Engineering Mechanics, Stanford University, Stanford, California, November 1960.

13. J. E. Gibson and D. B. Schultz, "The Variable Gradient Method of Generating Lyapunov Functions with Application to Automatic Control Systems," Control and Information Laboratory Report TREE 62-3, Purdue University, Lafayette, Indiana, April 1962.

14. G. P. Szegö, "On the Application of Lyapunov's Second Method to the Stability Analysis of Time-Invariant Control Systems," Control and Information Laboratory Report EE 62-9, Purdue University, Lafayette, Indiana, April 1962.

15. D. J. Wilde, Optimum Seeking Methods, Prentice-Hall, Englewood Cliffs, N. J., 1964.

16. G. A. Korn and T. M. Korn, Mathematical Handbook for Scientists and Engineers, McGraw-Hill, New York, 1961.

17. R. E. Kalman, "Mathematical Description of Linear Dynamical Systems," J.S.I.A.M. Control, Series A, Vol. 1, 2, pp. 152-192, 1963.

APPENDIX A. AREA CALCULATION

In order to compute the area within the curve V = constant for a second-order Lyapunov function of the form (3-3) it is convenient to transform the coordinates from the original x_1, x_2 system to a new y_1, y_2 system shown in Figure A-1. The transformation is performed by a rotation that positions the new y_1 axis perpendicular to the switching line.

The new coordinates may be expressed in terms of the angle of rotation θ as

$$\begin{bmatrix} y_1 \\ y_2 \end{bmatrix} = \begin{bmatrix} \cos\theta & \sin\theta \\ -\sin\theta & \cos\theta \end{bmatrix} \begin{bmatrix} x_1 \\ x_2 \end{bmatrix} \tag{A-1}$$

The switching line is defined by the equation

$$d_1 x_1 + d_2 x_2 = 0 \tag{A-2}$$

so that the unit normal vector to the switching line is given by

$$\underline{n} = \frac{1}{\sqrt{d_1^2 + d_2^2}} \begin{bmatrix} d_1 \\ d_2 \end{bmatrix} = \begin{bmatrix} \cos\theta \\ \sin\theta \end{bmatrix} \tag{A-3}$$

Define the matrix of the transformation as R :

$$\underline{y} = R\underline{x} \tag{A-4}$$

From (A-1) and (A-3), R is given by

$$R = \begin{bmatrix} \dfrac{d_1}{\sqrt{d_1^2 + d_2^2}} & \dfrac{d_2}{\sqrt{d_1^2 + d_2^2}} \\ \dfrac{-d_2}{\sqrt{d_1^2 + d_2^2}} & \dfrac{d_1}{\sqrt{d_1^2 + d_2^2}} \end{bmatrix} \tag{A-5}$$

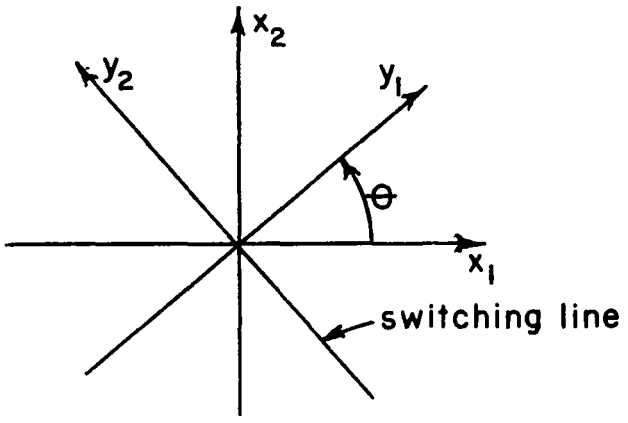

Fig. A-1 Two-Dimensional Coordinate Transformation.

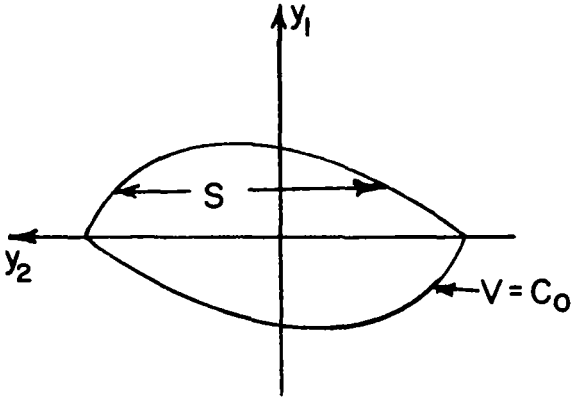

Fig. A-2 Definition of the Chord Length, S.

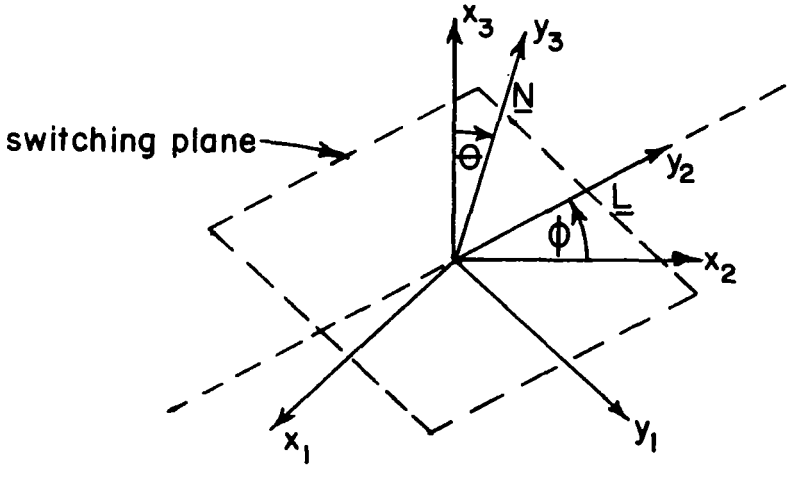

Fig. B-1 Three-Dimensional Coordinate Transformation.

In the original x coordinates the Lyapunov function is

$$V(\underline{x}) = \frac{1}{2}\,\underline{x}^T H \underline{x} + \underline{d}^T \underline{x} \tag{A-6}$$

In the new y coordinates this becomes

$$V(\underline{y}) = \frac{1}{2}\,\underline{y}^T R H R^T \underline{y} + (R\underline{d})^T \underline{y} \tag{A-7}$$

or

$$V(\underline{y}) = \frac{1}{2}\,\underline{y}^T G \underline{y} + \underline{p}^T \underline{y} \tag{A-8}$$

where

$$G = RHR^T \tag{A-9}$$

and

$$\underline{p} = R\underline{d} = \begin{bmatrix} \sqrt{d_1^2 + d_2^2} \\ 0 \end{bmatrix} \tag{A-10}$$

The equation

$$V(\underline{y}) = \text{constant} = C_0$$

becomes then

$$\frac{1}{2}\,G_{11}y_1^2 + \frac{1}{2}\,G_{22}y_2^2 + G_{12}y_1y_2 + p_1y_1 = C_0 \tag{A-11}$$

or, rearranging terms,

$$\left(\frac{1}{2}\,G_{22}\right)y_2^2 + \left(G_{12}y_1\right)y_2 + \left(-\,C_0 + p_1y_1 + \frac{1}{2}\,G_{11}y_1^2\right) = 0 \tag{A-12}$$

y_2 may be solved for from (A-12) to give

$$y_2 = -\,\frac{G_{12}}{G_{22}}\,y_1 \pm \sqrt{\left(\frac{G_{12}y_1}{G_{22}}\right)^2 - \frac{2\left(-\,C_0 + p_1y_1 + \frac{1}{2}\,G_{11}y_1^2\right)}{G_{22}}} \tag{A-13}$$

Figure A-2 shows the curve V = constant plotted in y coordinates. S is defined as the length of the chord joining two points on the curve on a line parallel to the y_2 axis. S is just twice the radical on the right of (A-13) or

$$S = 2\sqrt{\left(\frac{G_{12}y_1}{G_{22}}\right)^2 - \frac{2\left(-C_0 + p_1y_1 + \frac{1}{2}G_{11}y_1^2\right)}{G_{22}}} \qquad (A\text{-}14)$$

This can be rewritten as

$$S = \frac{2}{G_{22}}\sqrt{\left(G_{12}^2 - G_{11}G_{22}\right)y_1^2 - 2p_1G_{22}y_1 + 2C_0G_{22}} \qquad (A\text{-}15)$$

Define

$$a = G_{12}^2 - G_{11}G_{22} \qquad (A\text{-}16)$$

$$b = -2p_1G_{22} \qquad (A\text{-}17)$$

$$c = 2C_0G_{22} \qquad (A\text{-}18)$$

so that (A-15) becomes

$$S = \frac{2}{G_{22}}\sqrt{ay_1^2 + by_1 + c} \qquad (A\text{-}19)$$

Let U be the value of y_1 for which S = 0 .

$$U = -\frac{b}{2a} + \sqrt{\left(\frac{b}{2a}\right)^2 - \frac{c}{a}} \qquad (A\text{-}20)$$

The area within the curve defined by $V = C_0$ is

$$A = 2\int_0^U S\,dy_1 = \frac{4}{G_{22}}\int_0^U \sqrt{ax^2 + bx + c}\;dx \qquad (A\text{-}21)$$

Let

$$J = \int_0^U \sqrt{ax^2 + bx + c}\ dx \tag{A-22}$$

Integration by parts gives

$$J = \frac{2ax + b}{4a} \sqrt{ax^2 + bx + c}\ \Big|_0^U + \frac{4ac - b^2}{8a} \int_0^U \frac{dx}{\sqrt{ax^2 + bx + c}} \tag{A-23}$$

The integral in (A-23) may be evaluated from standard tables of integrals:

$$\int_0^U \frac{dx}{\sqrt{ax^2+bx+c}} = \begin{cases} \frac{1}{\sqrt{a}} \ln\left(2ax + b + 2\sqrt{a}\sqrt{ax^2+bx+c}\right) \Big|_0^U, & a > 0 \\ \frac{1}{\sqrt{-a}} \sin^{-1}\left(\frac{-2ax-b}{\sqrt{b^2-4ac}}\right) \Big|_0^U, & a < 0 \end{cases} \tag{A-24}$$

Let J_+ and J_- be the values of J corresponding to positive and negative values of a, respectively.

$$J_+ = \frac{-b\sqrt{c}}{4a} + \frac{4ac-b^2}{8a\sqrt{a}} \ln\left(2ax + b + 2\sqrt{a}\sqrt{ax^2+bx+c}\right) \Big|_0^U \tag{A-25}$$

$$J_- = \frac{-b\sqrt{c}}{4a} + \frac{4ac-b^2}{8a\sqrt{-a}} \sin^{-1}\left(\frac{-2ax-b}{\sqrt{b^2-4ac}}\right) \Big|_0^U \tag{A-26}$$

(A-25) may be written out as

$$J_+ = \frac{-b\sqrt{c}}{4a} + \frac{4ac-b^2}{8a\sqrt{a}} \left\{ \ln\left[b + 2a\left(\frac{-b}{2a} + \sqrt{\frac{b^2-4ac}{4a^2}}\right)\right] - \ln\left(b + 2\sqrt{ac}\right)\right\} \tag{A-27}$$

which simplifies to

$$J_+ = \frac{-b\sqrt{c}}{4a} + \frac{4ac-b^2}{8a\sqrt{a}}\,\ell n\left(\frac{\sqrt{b^2-4ac}}{(b+2\sqrt{ac})}\right) \qquad \text{(A-28)}$$

(A-26) may be written out as

$$J_- = \frac{-b\sqrt{c}}{4a} + \frac{4ac-b^2}{8a\sqrt{-a}}\left\{ \sin^{-1}\left[\frac{-2a}{\sqrt{b^2-4ac}}\left(\frac{-b}{2a} + \sqrt{\frac{b^2-4ac}{4ac^2}}\right) - \frac{b}{\sqrt{b^2-4ac}}\right] - \sin^{-1}\left(\frac{-b}{\sqrt{b^2-4ac}}\right)\right\} \qquad \text{(A-29)}$$

which simplifies to

$$J_- = \frac{-b\sqrt{c}}{4a} + \frac{4ac-b^2}{8a\sqrt{-a}}\left[\sin^{-1}(+1) - \sin^{-1}\left(\frac{-b}{\sqrt{b^2-4ac}}\right)\right] \qquad \text{(A-30)}$$

Noting that

$$\sin^{-1}w = \tan^{-1}\frac{w}{\sqrt{1-w^2}} \qquad \text{(A-31)}$$

(A-30) may be rewritten as

$$J_- = \frac{-b\sqrt{c}}{4a} + \frac{4ac-b^2}{8a\sqrt{a}}\left[1.57079632 - \tan^{-1}\left(\frac{-b}{\sqrt{4|a|c}}\right)\right] \qquad \text{(A-32)}$$

(A-28) and (A-32) finally become, after a little rewriting,

$$J_+ = \frac{b^2-4ac}{8|a|\sqrt{|a|}}\,\ell n\left(\frac{b+\sqrt{4|a|c}}{\sqrt{b^2-4ac}}\right) - \frac{b\sqrt{c}}{4a} \qquad \text{(A-33)}$$

$$J_- = \frac{b^2-4ac}{8|a|\sqrt{|a|}}\left[1.57079632 - \tan^{-1}\left(\frac{-b}{\sqrt{4|a|c}}\right)\right] - \frac{b\sqrt{c}}{4a} \qquad \text{(A-34)}$$

The total area is then given simply by

$$A = \frac{4}{G_{22}}J \qquad \text{(A-35)}$$

where

$$J = \begin{cases} J_+ , & a > 0 \\ J_- , & a < 0 \end{cases}$$

APPENDIX B. VOLUME CALCULATION

B-1. TRANSFORMATION OF COORDINATES

Consider a third-order Lyapunov function of the form (3-3) as a function of orthogonal coordinates x_1, x_2, x_3. It will be convenient to compute the volume contained within the surface V = constant in a new orthogonal coordinate system, two of whose axes lie on the switching plane. The area of the (elliptical) cross section parallel to the switching surface can then easily be computed and integrated to obtain the volume.

Let the coordinates of the new system be given by y_1, y_2, y_3. Let $\underline{L}$ be a vector determined by the intersection of the switching plane and the x_2-x_3 plane, and let $\underline{N}$ be a vector normal to the switching plane. The sketch in Figure B-1 illustrates the geometry. The transformation from x to y coordinates is chosen to be, for simplicity, first a rotation about the x_3 axis by an angle φ to line up the x_2 axis with $\underline{L}$, and then finally a rotation about $\underline{L}$ by an angle θ to line the x_3 axis up with $\underline{N}$.

Let the vectors $\underline{L}$ and $\underline{N}$ be given by

$$\underline{N} = \begin{bmatrix} d_1 \\ d_2 \\ d_3 \end{bmatrix} \tag{B-1}$$

and

$$\underline{L} = \underline{k} \times \underline{N} = \begin{bmatrix} -d_2 \\ d_1 \\ 0 \end{bmatrix} \tag{B-2}$$

(where $\underline{k}$ is the unit vector on the x_3 axis).

The first rotation produces a coordinate set x_1', x_2', x_3', given by

$$\begin{bmatrix} x_1' \\ x_2' \\ x_3' \end{bmatrix} = \begin{bmatrix} \cos\varphi & \sin\varphi & 0 \\ -\sin\varphi & \cos\varphi & 0 \\ 0 & 0 & 1 \end{bmatrix} \begin{bmatrix} x_1 \\ x_2 \\ x_3 \end{bmatrix} \tag{B-3}$$

The second rotation produces the desired set

$$\begin{bmatrix} y_1 \\ y_2 \\ y_3 \end{bmatrix} = \begin{bmatrix} \cos\theta & 0 & -\sin\theta \\ 0 & 1 & 0 \\ \sin\theta & 0 & \cos\theta \end{bmatrix} \begin{bmatrix} x_1' \\ x_2' \\ x_3' \end{bmatrix} \tag{B-4}$$

The complete transformation is then given by a successive application of (B-3) and (B-4) as

$$\begin{bmatrix} y_1 \\ y_2 \\ y_3 \end{bmatrix} = \begin{bmatrix} \cos\theta\cos\varphi & \cos\theta\sin\varphi & -\sin\theta \\ -\sin\varphi & \cos\varphi & 0 \\ \cos\varphi\sin\theta & \sin\theta\sin\varphi & \cos\theta \end{bmatrix} \begin{bmatrix} x_1 \\ x_2 \\ x_3 \end{bmatrix} \tag{B-5}$$

$$\underline{y} = R\underline{x} \tag{B-6}$$

The application of a little geometry shows that

$$\cos\varphi = d_1 \Big/ \sqrt{d_1^2 + d_2^2}$$

$$\cos\theta = d_3 \Big/ \sqrt{d_1^2 + d_2^2 + d_3^2}$$

$$\sin\varphi = d_2 \Big/ \sqrt{d_1^2 + d_2^2}$$

$$\sin\theta = \sqrt{d_1^2 + d_2^2} \Big/ \sqrt{d_1^2 + d_2^2 + d_3^2} \tag{B-7}$$

Setting

$$z_1 = \sqrt{d_1^2 + d_2^2 + d_3^2} \tag{B-8}$$

and

$$z_2 = \sqrt{d_1^2 + d_2^2} \tag{B-9}$$

we can write R as

$$R = \frac{1}{z_1} \begin{bmatrix} d_1 d_3/z_2 & d_2 d_3/z_2 & -z_2 \\ -d_2 z_1/z_2 & d_1 z_1/z_2 & 0 \\ d_1 & d_2 & d_3 \end{bmatrix} \tag{B-10}$$

B-2. TRANSFORMATION OF THE LYAPUNOV FUNCTION

The Lyapunov function in the old coordinates is given by

$$\frac{1}{2} \underline{x}^T H \underline{x} + \underline{d}^T \underline{x} = C_0 \tag{B-11}$$

In the new coordinates, after the transformation $\underline{y} = R\underline{x}$, it becomes

$$\frac{1}{2} \underline{y}^T G \underline{y} + \underline{p}^T \underline{y} = C_0 \tag{B-12}$$

where

$$G = RHR^T \tag{B-13}$$

and

$$\underline{p} = R\underline{d} \tag{B-14}$$

B-3. COMPUTATION OF THE AREA OF A CROSS-SECTION OF (B-12)*

Rewrite (B-12) in terms of y_1 and y_2 with y_3 considered as

*Alternate expressions for the area may be derived using the invariants of a quadratic form; see, for example, Reference [16].

a parameter (y_3 is the coordinate normal to the switching plane):

$$\frac{1}{2}\begin{bmatrix} y_1 \\ y_2 \end{bmatrix}^T \begin{bmatrix} G_{11} & G_{12} \\ G_{12} & G_{22} \end{bmatrix} \begin{bmatrix} y_1 \\ y_2 \end{bmatrix} + \underline{k}^T \begin{bmatrix} y_1 \\ y_2 \end{bmatrix} = C_1 \qquad \text{(B-15)}$$

where

$$\underline{k} = \begin{bmatrix} p_1 + G_{13}y_3 \\ p_2 + G_{23}y_3 \end{bmatrix} \qquad \text{(B-16)}$$

and

$$C_1 = C_0 - \frac{1}{2} G_{33}y_3^2 - p_3y_3 \qquad \text{(B-17)}$$

Define $\hat{G}$ to be the matrix of the quadratic form (B-15),

$$\hat{G} = \begin{bmatrix} G_{11} & G_{12} \\ G_{12} & G_{22} \end{bmatrix} \qquad \text{(B-18)}$$

The eigenvalues of $\hat{G}$ are

$$\lambda_1 = \frac{G_{11} + G_{22}}{2} + \sqrt{\left(\frac{G_{11}+G_{22}}{2}\right)^2 + G_{12}^2 - G_{11}G_{22}} \qquad \text{(B-19)}$$

$$\lambda_2 = \frac{G_{11} + G_{22}}{2} - \sqrt{\left(\frac{G_{11}+G_{22}}{2}\right)^2 + G_{12}^2 - G_{11}G_{22}} \qquad \text{(B-20)}$$

The transformation matrix, M, which transforms $\hat{G}$ to the diagonal form

$$M^T \hat{G} M = \begin{bmatrix} \lambda_1 & 0 \\ 0 & \lambda_2 \end{bmatrix} \qquad \text{(B-21)}$$

may be solved for as follows:

Let M be the matrix whose columns are the normalized eigenvectors of $\hat{G}$,

$$M = \left[\underline{u}^1 , \quad \underline{u}^2 \right] \tag{B-22}$$

$$\hat{G}\underline{u}^i = \lambda_i \underline{u}^i , \qquad i = 1,2 \tag{B-23}$$

$$(u_1^i)^2 + (u_2^i)^2 = 1 , \qquad i = 1,2 \tag{B-24}$$

From (B-23)

$$u_1^i = \frac{G_{12}}{\lambda_1 - G_{11}} u_2^i \tag{B-25}$$

Using (B-25), (B-24), and (B-22) we solve for M, after defining

$$Q_i = \frac{G_{12}}{\lambda_i - G_{11}} \tag{B-26}$$

$$M = \begin{bmatrix} \dfrac{Q_1}{\sqrt{1 + Q_1^2}} & \dfrac{Q_2}{\sqrt{1 + Q_2^2}} \\ \dfrac{1}{\sqrt{1 + Q_1^2}} & \dfrac{1}{\sqrt{1 + Q_2^2}} \end{bmatrix} \tag{B-27}$$

The transformed variables z_1, z_2 are given by

$$\begin{bmatrix} z_1 \\ \\ z_2 \end{bmatrix} = M^T \begin{bmatrix} y_1 \\ \\ y_2 \end{bmatrix} \tag{B-28}$$

so that (B-15) becomes

$$\frac{1}{2} \lambda_1 z_1^2 + \frac{1}{2} \lambda_2 z_2^2 + \underline{k}^T M \underline{z} = C_1 \tag{B-29}$$

Define

$$\underline{w} = M^T \underline{k} \tag{B-30}$$

(B-29) can be rewritten, after completing squares, as

$$\frac{1}{2}\lambda_1\left(z_1 + \frac{w_1}{\lambda_1}\right)^2 + \frac{1}{2}\lambda_2\left(z_2 + \frac{w_1}{\lambda_2}\right)^2 = C_1 + \frac{w_1^2}{2\lambda_1} + \frac{w_2^2}{2\lambda_2} \tag{B-31}$$

or

$$\frac{\left(z_1 + \frac{w_1}{\lambda_1}\right)^2}{\frac{2}{\lambda_1}\left(C_1 + \frac{w_1^2}{2\lambda_1} + \frac{w_2^2}{2\lambda_2}\right)} + \frac{\left(z_2 + \frac{w_2}{\lambda_2}\right)^2}{\frac{2}{\lambda_2}\left(C_1 + \frac{w_1^2}{2\lambda_1} + \frac{w_2^2}{2\lambda_2}\right)} = 1 \tag{B-32}$$

The area of an ellipse with minor and major semi-axes a and b is

$$A = \pi ab \tag{B-33}$$

For the elliptical section described by (B-32) we have

$$a = \sqrt{\frac{2}{\lambda_1}\left(C_1 + \frac{w_1^2}{2\lambda_1} + \frac{w_2^2}{2\lambda_2}\right)} \tag{B-34}$$

and

$$b = \sqrt{\frac{2}{\lambda_2}\left(C_1 + \frac{w_1^2}{2\lambda_1} + \frac{w_2^2}{2\lambda_2}\right)} \tag{B-35}$$

so that the area is

$$A = \frac{2\pi}{\sqrt{\lambda_1\lambda_2}}\left(C_1 + \frac{w_1^2}{2\lambda_1} + \frac{w_2^2}{2\lambda_2}\right) \tag{B-36}$$

From (B-27) and (B-30),

$$w_1 = \frac{1}{\sqrt{1 + Q_1^2}} (k_1 Q_1 + k_2) \tag{B-37}$$

$$w_2 = \frac{1}{\sqrt{1 + Q_2^2}} (k_1 Q_2 + k_2) \tag{B-38}$$

Substituting (B-37) and (B-38) in (B-36) and using (B-16) to eliminate k_1 and k_2 we obtain

$$A = \frac{2\pi}{\sqrt{\lambda_1 \lambda_2}} (S_1 y_3^2 + S_2 y_3 + S_1) \tag{B-39}$$

where

$$S_1 = \sum_{i=1}^{2} \frac{(Q_i G_{13} + G_{23})^2}{2\lambda_i (1 + Q_i^2)} - \frac{1}{2} G_{33} \tag{B-40}$$

$$S_2 = \sum_{i=1}^{2} \frac{(Q_i p_1 + p_2)(Q_i G_{13} + G_{23})}{\lambda_i (1 + Q_i^2)} - p_3 \tag{B-41}$$

$$S_3 = \sum_{i=1}^{2} \frac{(Q_i p_1 + p_2)^2}{2\lambda_i (1 + Q_i^2)} + C_0 \tag{B-42}$$

B-4. COMPUTATION OF THE VOLUME

One half of the volume contained in $V = C_0$ is obtained by integrating (B-39) from $y_3 = 0$ to the extremity of the bounding surface. The upper limit, U, is obtained by setting $A = 0$ in (B-39) and solving for y_3:

$$U = -\frac{S_2}{2S_1} \pm \sqrt{\left(\frac{S_2}{2S_1}\right)^2 - \frac{S_3}{S_1}} \tag{B-43}$$

The total volume is then given by

$$2\int_0^U A\,dy_3 \tag{B-44}$$

or

$$\text{Volume} = \frac{4\pi}{\sqrt{\lambda_1\lambda_2}}\left(\frac{S_1}{3}U^3 + \frac{S_2}{2}U^2 + S_3U\right) \tag{B-45}$$